



**HAL**  
open science

# A surrogate deterioration model of debris retention systems towards cost-effective maintenance strategies and increased protection efficacy

Nour Chahrour, Guillaume Piton, Jean-Marc Tacnet, Christophe Bérenguer

## ► To cite this version:

Nour Chahrour, Guillaume Piton, Jean-Marc Tacnet, Christophe Bérenguer. A surrogate deterioration model of debris retention systems towards cost-effective maintenance strategies and increased protection efficacy. *Engineering Structures*, 2024, 300, pp.117202. 10.1016/j.engstruct.2023.117202 . hal-04304170

**HAL Id: hal-04304170**

**<https://hal.science/hal-04304170v1>**

Submitted on 29 Nov 2023

**HAL** is a multi-disciplinary open access archive for the deposit and dissemination of scientific research documents, whether they are published or not. The documents may come from teaching and research institutions in France or abroad, or from public or private research centers.

L'archive ouverte pluridisciplinaire **HAL**, est destinée au dépôt et à la diffusion de documents scientifiques de niveau recherche, publiés ou non, émanant des établissements d'enseignement et de recherche français ou étrangers, des laboratoires publics ou privés.



Distributed under a Creative Commons Attribution - NonCommercial - NoDerivatives 4.0 International License

# A Surrogate Deterioration Model of Debris Retention Systems Towards Cost-Effective Maintenance Strategies and Increased Protection Efficacy

Nour Chahrour<sup>a,b,\*</sup>, Guillaume Piton<sup>a</sup>, Jean-Marc Tacnet<sup>a</sup> and Christophe Bérenguer<sup>b</sup>

<sup>a</sup>Univ. Grenoble Alpes, INRAE, ETNA, 38000 Grenoble, France.

<sup>b</sup>Univ. Grenoble Alpes, CNRS, Grenoble INP, GIPSA-lab, 38000 Grenoble, France.

---

## ARTICLE INFO

### Keywords:

deterioration trajectories  
maintenance optimization  
protection efficacy  
stochastic Petri nets  
debris retention system  
debris flows

## ABSTRACT

Protection systems are usually implemented in mountains aiming to resist natural dangerous phenomena. As any other critical infrastructure, protection systems should always withstand and operate efficiently as they guarantee the safety of people and protect socio-economic assets. However, the efficacy of these systems decreases with the increase of the deterioration level of the interdependent components, which constitute them. To provide desirable operation over their lifetime, the management of protection systems is of paramount importance. A major key issue in such critical infrastructure management is to optimize the cost effectiveness of maintenance actions while maintaining a sufficient protection efficacy. This study proposes a decision-aiding model to assess different maintenance strategies applied to a protection system against debris flows. The model is constructed using physics-based stochastic Petri nets. It incorporates (1) a stochastic deterioration model, which is a surrogate model of a physics-based model developed for building deterioration trajectories of the system and (2) maintenance model that permits assessing the cost and efficiency of maintenance strategies. This study addresses the case of a debris retention system, in which the progressive filling of its basin by debris materials is modeled. This is followed by assessing several maintenance strategies concerning the cleaning of the basin. A simple sensitivity analysis is also carried out in order to check the effect of the uncertainty that invades the model's inputs on maintenance decisions. A numerical analysis is performed using real data of the retention system located in the Claret torrent in France and subjected to debris flows over a period of 50 years.

---

## 1. Introduction

### 1.1. Infrastructure Asset Management & Decision Support Systems

Reliable, operational and durable infrastructure assets are essential for economic prosperity in the modern society (Biondini and Frangopol, 2016). Foremost, asset management aims to maintain infrastructures in acceptable conditions that permit them to fulfill their desired functional objectives (Asghari and Hsu, 2021). Indeed, the aging, loading and environmental factors in addition to natural and man-made hazards continuously influence the condition of these infrastructure systems. The process of infrastructure asset management starts by condition monitoring, data collection, information analysis and ends with decision-making concerning maintenance plans.

Efficacy assessment depends on dynamic and reliable monitoring and evaluation of deterioration indicators. Otherwise, poor assessment, misjudgments and bad decisions will be made. Nonetheless, recent advances make it possible to integrate information technology such as artificial intelligence (AI) techniques (Russell and Norvig, 2020) and decision support systems (DSS) (Bonczek et al., 1981) to enhance and enrich decision-making processes. Through gathering real-time data, analyzing data trends, providing forecasts and quantifying uncertainty, an intelligent decision support system can provide reliable insights that support decision-makers to make optimal management decisions.

Definitely, the use of AI and DSS methods in infrastructure management is not new. They have been and are still being used in different disciplines as a crucial part of the decision-making process. The novelty lies in the challenge of developing such techniques in order to support a more holistic approach toward dynamic and compelling management decisions. For structural engineering applications (e.g., highways, bridges, dams), AI and DSS methods have been

---

\*Corresponding author

✉ [nour.chahrour@inrae.fr](mailto:nour.chahrour@inrae.fr) (N. Chahrour)

ORCID(s): 0000-0003-2982-3169 (N. Chahrour)

adopted for deterioration modeling and maintenance optimization (Šelih et al., 2008; Callow et al., 2012; Guler, 2013; Pan and Zhang, 2021; Yang et al., 2022; Wang et al., 2021).

## 1.2. Management of Torrent Protection Systems

Torrential watersheds are located in mountains and are usually exposed to different types of natural phenomena such as torrential floods and debris flows carrying not only water but also huge volumes of debris (Coussot and Meunier, 1996). These phenomena induce risk in downstream areas where vulnerable assets are located (people, houses, roads, etc.). They trigger casualties, injuries, destruction and economic damages (Hilker et al., 2009; Badoux et al., 2014). Since the 19<sup>th</sup> century, engineers started implementing different types of protection systems (check dams, debris retention systems, dykes) along watersheds seeking to reduce the risk level generated by torrential phenomena. These systems aim in fulfilling essential functions that provide protection either by reducing the causes of the phenomena, e.g., erosion at source areas, or by reducing its consequences, e.g., deposition, overflows (Piton et al., 2017). However, during their lifetime, they are exposed to high intensity phenomena and damaging events that trigger their deterioration.

Visual inspection remains the most common technique used to identify the level of deterioration of protection systems and to assign accordingly a maintenance operation. While it does offer the advantage of seeing the damages in real, visual inspection depends on inspectors (experts, engineers, or technicians) who capture photographs, interpret them and write reports. The latter then becomes the main source of information used by the managers of these systems to optimize their maintenance strategies. Nevertheless, field inspections are difficult due to the particular constraints in mountain regions (remote structures, isolation, extreme weather, high altitudes and rough terrain). In addition, in France, limited budgets are provided by the State for the management of protection systems. This highlights the importance to develop decision support models that use, merge and analyze available information in order to prioritize inspection and maintenance plans to be carried out on systems that require rehabilitation.

The present study focuses on the management of debris retention systems as they exist in most French torrents and their deterioration could lead to dramatic consequences on vulnerable issues exposed to torrential phenomena.

## 1.3. Debris Retention Systems: Design & Maintenance Experience

Debris retention systems are among the most adopted torrent protection systems in Europe (e.g., Alps) and Asia (e.g., Japan) in torrents highly exposed to debris flows (Zollinger, 1985; Ikeya, 1989). Roughly speaking, these structures seek to trap debris before they reach areas where their deposition may aggravate the damage. These systems are usually composed of separate components (fig. 1), each having its own functions but all working collaboratively on increasing the efficacy of the overall system in providing a high level of protection. The basic components that must at least be present are a debris basin, a retention dam and a maintenance access track. The access track allows trucks to access the debris basin to carry out maintenance operations on the different components. The debris basin is a deposition area where solid materials (boulders, sediments and woody debris) are stored. It is characterized by its storage capacity defined. In addition, at the outlet of the basin, a retention dam regulates torrential flows leaving the basin by filtering and trapping solid materials. The type, shape and size of the system's components may differ from one torrent to another depending on its characteristics and on the desired functional requirements (Hübl and Suda, 2008).

From an operational point of view, debris retention systems usually aim to fulfill the following functions (Zollinger, 1985; Armanini et al., 1991; Hübl et al., 2005):

*Filtering the flow:* sorting and storing solid materials based on their size and severity (e.g., large boulders). This function is used on sites where large transported elements could jam the channel (e.g., at bridges or culverts).

*Buffering the flow:* regulating the flow by storing temporarily a specific volume of the flow and then self-cleaning by releasing this volume with a lower discharge to downstream areas. This function is used on sites where channel overflowing occurs for excess peak discharge.

*Debris deposition:* trapping of a given volume of sediment that will not be released naturally and must be removed with excavators to recover the structure capacity. This function is used on sites where channel overflowing occurs because of chronic deposition when too much sediment is supplied by the catchment.

Most debris basins are used to target the latter function but the progress in debris flow hazard assessments enables to identify catchments where the two first functions are more suitable: more effective, less costly and with fewer side effects (Hübl, 2018). Understanding the structural design of debris retention systems in addition to the desired



**Figure 1:** Multi-component retention system: (1) retention dam; (2) debris basin; (3) access track; (4) lateral dykes; (5) downstream counter dam. Claret retention system, France. © ONF-RTM/S. Carladous May, 23<sup>rd</sup> 2018.

functional objectives that must be fulfilled facilitates identifying possible failure modes that lead to the partial or total destruction or malfunctioning of the entire system. A recent study reviewed the French experience with debris retention systems, thus providing a thorough review concerning their malfunctions and maintenance issues (Carladous et al., 2022). The failure modes observed or expected to occur were reported on 115 existing debris retention systems implemented in French massifs. One of the most frequently observed types of failures is the excess of trapping in the basin (reported in about one-third of the structures). It is mostly triggered by the jamming of the dam's openings by boulders and large woody debris. This excess of sediment trapping is fixed at high costs by regular cleaning operations. In a few cases, the structures were adapted to be more rarely obstructed but this option may change the protection efficacy (Carladous et al., 2022).

In French torrents, the monitoring of debris retention systems is currently largely based either on field inspection or on expert appraisal processes during which technicians imagine the evolution of a deterioration indicator (e.g., trapped volume in the debris basin) in the short, medium and long term by combining several scenarios related to physical phenomena. On these bases, maintenance decisions are made. Indeed, managers have adopted specific maintenance policies based on the torrent. Particularly, for some torrents, each time a debris flow occurs, they ask for scheduling maintenance where all the stored volume in the debris basin should be cleaned. In other torrents, cleaning operations are scheduled depending on the stored volume of solid materials in the basin. This depends on the activity of the torrent, on the vulnerability of the assets to be protected in downstream and on available budgets.

#### 1.4. Objectives and Main Scientific Contributions

Excessive maintenance costs can also be seen as a malfunction. Therefore, a properly defined and implemented maintenance policy can improve the resilience of complex infrastructure systems. Indeed, it is important to carefully address the inspection frequency and to differentiate between different maintenance strategies. This in turn necessitates acquiring a comprehensive knowledge on the dynamic behavior of the deteriorating system as well as on the protection efficacy in its various states of deterioration (i.e., filling in the case of debris basins). In industrial and technological systems, monitoring is common. However, as mentioned in section 1.2, protection systems in mountains are not well instrumented and are not easily reached. Therefore, there is a lack of sufficient deterioration data to build time-dependent deterioration trajectories.

Physical models that study the deterioration mechanisms of a system when subjected to undesirable events over time provide essential information for building deterioration trajectories. However, such models couple several sub-models that represent the complex interdependent physical phenomena related to the field of study (e.g., sediment transport, hydraulics, structural behavior). This issue makes the physical model too complicated to be used directly in a decision-making process. On the other hand, reliability-maintenance tools such as stochastic Petri nets (SPNs) (Signoret, 2009; Aubry et al., 2016) implementing condition-based maintenance policy (CBM) (Alaswad and Xiang, 2017) offer a flexible and efficient model to support decision-making. Such a model represents the stochastic deterioration of the system relying only on probability laws associated with transitions from one deteriorated state to another. However, it does not reflect the physics behind this deterioration process.

In essence, the main contribution behind this research work is to optimize maintenance decisions of deteriorating protection systems by leveraging and coupling two domains: (1) scenario-driven physics-based modeling, which provides valuable information concerning the physical process behind the deterioration mechanisms of the system as well as its protection efficacy and (2) reliability-based modeling using SPNs, which provides a simpler representation of the physical deterioration process and makes it possible to easily implement a CBM policy in it. In other words, the objective is to develop a reliability-based model as a surrogate model of the scenario-driven physics-based model by using the information provided by the latter.

A very recent model-based decision support system was developed in order to optimize maintenance strategies of deteriorating check dams subjected to torrential floods (Chahrour et al., 2021). The developed approach physically models the deterioration of a check dam only from a structural point of view (loss in external stability) and uses SPN tools in order to support maintenance decision-making considering only economic aspects. In this paper, we extend this previous work to support maintenance decision-making of debris retention systems. In comparison to the work performed in Chahrour et al. (2021), the present study aims to support maintenance decision-making of debris retention systems, which are completely different than check dams in terms of functional and structural characteristics. The novelty of this work lies in: (1) developing a scenario-driven physics-based model that studies the deterioration of a debris retention system from a functional, rather than structural, point of view; (2) developing a SPN model that makes it possible to assess maintenance strategies considering economic aspects but also the efficiency of the strategies in increasing the protection efficacy provided by the system; and (3) exploring different assumptions (e.g., different inspection frequency, maintenance duration, maintenance cost) in order to check whether the results regarding maintenance decisions would be the same or not in different situations.

The research carried out in this paper is multidisciplinary and develops contributions in different domains. In the context of natural risks and protection systems, the time-dependent behavior of a system is a recent field of study. Chahrour et al. (2021) was the first who deal with this issue starting with the case of check dams. Meanwhile, Piton et al. (2022) recently developed a comprehensive way to model the routing of debris flows through debris retention systems. However, the model was applied to only two debris flow events resulting in a static view of the system's state. In this study, the model is developed further so that it considers series of debris flow events and it models the dynamic evolution of the physical model's output parameters (e.g., jamming rate of the dam's openings, stored volume in the basin) when subjected to those events. The principle is to analyze failure scenarios through physics-based modeling, in which available information acquired from different sources is merged and used. Besides, in the context of protection system management, the developed scenario-driven physics-based model contributes in providing unavailable knowledge about deterioration trajectories of debris retention systems. Regarding maintenance management of complex systems, the developed SPN model contributes in supporting the managers of these systems to better anticipate and make optimal decisions. Last but not least, the overall surrogate model-based decision support system developed in this study is a totally generic approach that can be used to manage the operation and maintenance of any engineering system/structure thus contributing to improved resilience of constructed systems and/or to improved designs of future constructions, relying on automation instead of human intervention.

The paper is structured as follows: Section 2 presents the overall developed methodological approach. It starts by building deterioration trajectories corresponding to the filling of a debris basin over time through scenario-driven physics-based modeling and then using these trajectories in the developed SPN model for supporting maintenance decision-making. Section 3 describes a real case study: the debris retention system located in the Claret torrent in France. Section 4 provides the numerical outputs resulting after modeling the considered case study using the developed approach. Conclusion and perspectives are presented in section 5.

## 2. Developed Methodological Approach

This section represents the methodological contribution. It provides a detailed description of the integrated approach used to tackle the identified scientific and technical obstacles.

### 2.1. Global Framework Description

The objective of this work is to analyze the dynamic behavior of a debris retention system when subjected to debris flows over its lifetime. The analysis concerns the failure of the system due to the excess storage in its debris basin. This type of failure is so common for retention systems and it usually requires regular maintenance operations. It is a functional failure, which deprives the system from achieving its function in buffering the flow (releasing the

stored volume with low discharge). Indeed, as the volume stored in the basin increases, the efficacy of the system in providing protection by trapping material decreases. In order to model the filling of a debris basin over time, an integrated approach is developed. The overall modeling approach (fig. 2) can be summarized by the following steps, which are detailed in the next subsections.

1. *Retention system and debris flow features' definition (fig. 2a)*: describing the dam, its openings and the basin's storage capacity in addition to defining the features of the debris flow events that occur (e.g., hydrographs, transported boulders).
2. *Debris flow scenarios generation (fig. 2b)*: creating virtual series of debris flow events with defined dates of occurrence and volumes over a specified period of time (calibrated with observed time series if available).
3. *Events' consequences and resulting failure analysis (fig. 2c)*: modeling the evolution of the debris volume stored in the basin  $V_b$  ( $m^3$ ) after each debris flow event. The model should explicitly take into consideration the jamming of the retention dam's openings by transported boulders over time. This is due to the fact that as the jamming rate increases, the discharge capacity of the dam decreases and thus  $V_b$  increases.
4. *Stochastic deterioration and maintenance modeling (fig. 2d)*: proposing  $V_b$  as a deterioration indicator, defining deterioration states corresponding to the state of filling of the debris basin, estimating empirical non-parametric probability laws corresponding to transition times between those states using the obtained deterioration trajectories of  $V_b$  and modeling the stochastic behavior of the system when subjected to deterioration mechanisms (progressive or rapid filling of the basin) and to maintenance operations (cleaning of the basin).

## 2.2. Scenario-Driven Physics-Based Model: Debris Flows Routing through Retention Systems

Debris retention systems are designed to mitigate natural risk by storing a specific volume of a debris flow in the debris basin and then releasing it to downstream areas with an acceptable discharge. On one hand, storing low magnitude events increases the stored volume in the basin thus reducing its capacity. On the other hand, the passage of high magnitude events through the retention dam may pose a threat to downstream exposed issues. Consequently, a sufficiently fine understanding of the physical process corresponding to the routing of debris flows through a retention system is essential to optimize the efficacy of the system in providing protection and to avoid unnecessary costs of cleaning operation. For this purpose, a scenario-driven physics-based model is developed. The end purpose of the model is to build deterioration trajectories corresponding to the evolution of the stored volume in a debris basin over time. The model consists of several sequential stages, presented in the following subsections.

### 2.2.1. Step 0: Data Acquisition and Generation of Random Debris Flows Scenarios

Several input data should be acquired for launching simulations. Indeed, the model requires knowledge concerning the (i) geometry of the retention dam (shape, dimensions, openings), (ii) characteristics of the debris basin (storage capacity, deposition slope, stage-volume capacity curve) and (iii) debris flows characteristics (return periods, inlet hydrographs, size and number of transported boulders). Some of these data can be extracted from the historical database and topographical surveys while others could be missing and have to be assumed or obtained by modeling.

In debris basins, deposition does not occur horizontally. The deposition slope depends on the sediment concentration and on the type of sediment transport. The stage-volume capacity curve depends on the deposition slope and provides an estimate of the volume of debris stored in the basin below a specific level at the dam (fig. 2a). In addition, the inlet hydrograph represents the inlet discharge of the debris flow event as a function of time. In case available data are limited, triangular hydrographs can be assumed. In this case, the hydrograph can be described by four parameters: the debris flow volume  $V_{event}$ , peak discharge  $Q_{peak}$ , time to peak  $t_{peak}$  and time to end  $t_{end} = 2 \cdot V_{event} / Q_{peak}$  (fig. 2a).

Usually, the volume of the debris flow event  $V_{event}$  is defined from frequency – magnitude analyses and  $Q_{peak}$  is estimated based on empirical equations as Eq. (1) proposed by Mizuyama et al. (1992).

$$Q_{peak} = 0.0188 \cdot V_{event}^{0.79} \quad (1)$$

Debris flow scenarios, i.e., series of debris flow events characterized by their date  $D_{event}$  and volumes  $V_{event}$  should be generated to feed the physics-based model. These random variables can be randomly sampled based on historical archives concerning the magnitude (volume) and the frequency (probability) of debris flow events that have already occurred in the studied torrent. The generated scenarios will be fed separately to the model and the events involved in

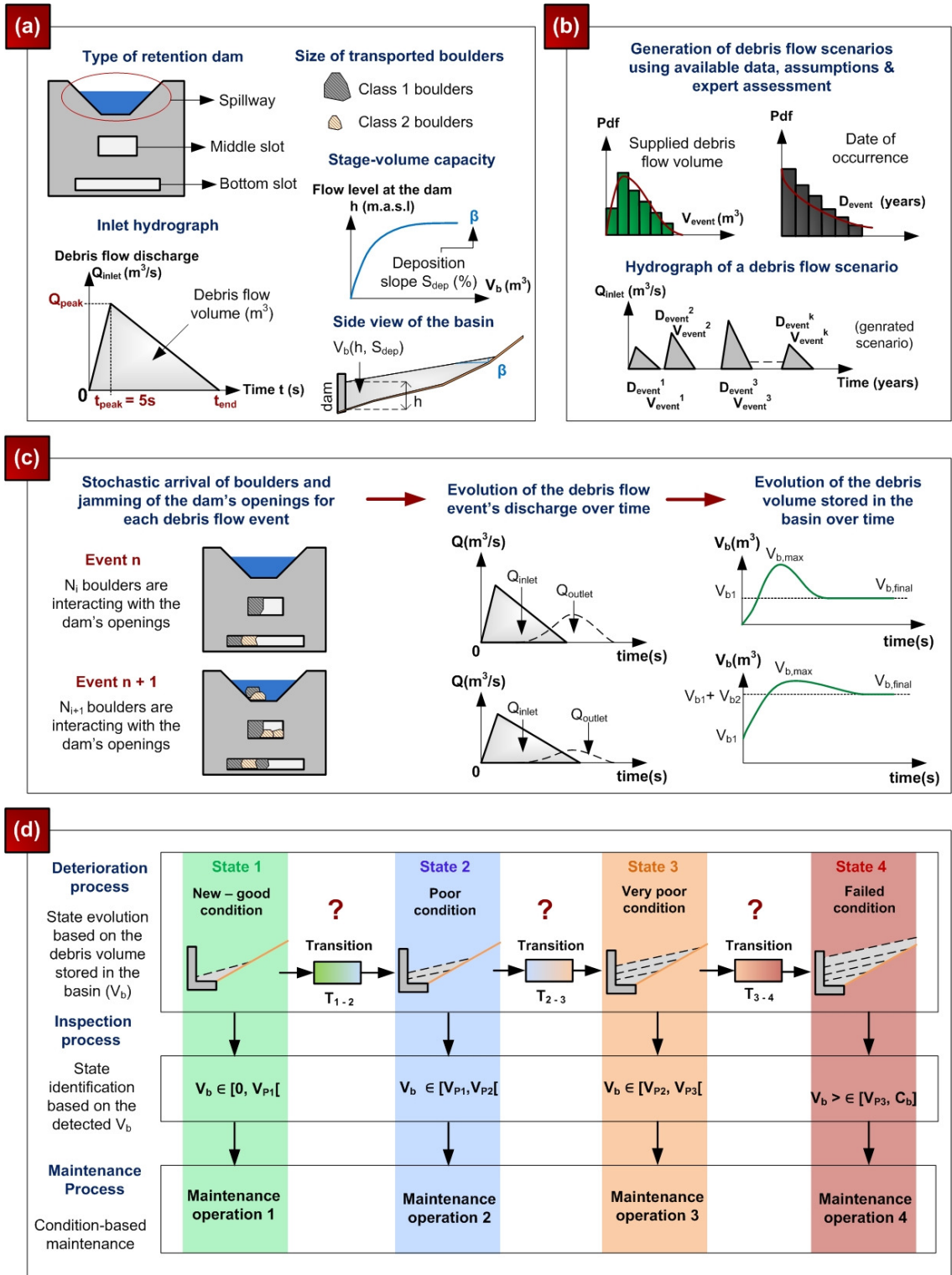


**Figure 2:** Key steps of the modeling process of a debris retention system: (a) system's geometry and debris flows features; (b) debris flow scenarios; (c) resulting failures and flow routing analysis and (d) stochastic deterioration and maintenance modeling.



The total outlet discharge  $Q_{outlet}$  released through the openings of a retention dam is equal to the sum of the discharge capacities through the  $I$  openings of the dam.

$$Q_{outlet}(t) = \sum_{i=1}^I Q_i(t) \quad (4)$$

### 2.2.3. Step 2: Jamming Conditions and Stochastic Arrival of Boulders

In order to assess possible interactions between transported boulders and the retention dam's openings, simple hydraulic approaches that provide the spatio-temporal distribution of boulders approaching the dam and predict whether or not the boulders jam the dam's openings should be developed. A very recent model that analyzes the (i) conditions of jamming based on granular dynamics and (ii) the stochastic arrival of boulders to the dam was proposed by Piton et al. (2022). This model is used as a sub-model in the overall approach developed in this paper. To conduct this study, we made a specific adjustment compared to the original model. We changed only the initial state of the basin's filling when a new event occur, with this initial state being set based on the filling level at the end of the previous event (empty basin for the first event). It is worth noting that the original model was primarily designed for analyzing isolated events, whereas our current work focuses on a series of events. Apart from this distinction, the two models are similar. A brief description of this sub-model is presented below.

The jamming process of a retention dam's openings is governed by the size of boulders relative to the size of the openings. The dam's openings can be jammed based on three different arrangements:

- *Lateral jamming* occurs when the following condition is satisfied (e.g., middle slot in fig. 3):

$$D_A + D_B > w_i(t) \quad (5)$$

where  $D_A$  and  $D_B$  are the diameters of the two largest boulders passing together at time  $t$  through the opening number  $i$  and  $w_i(t)$  is the free width of opening  $i$  at time  $t$ .

- *Vertical jamming* occurs only when the diameter of a boulder is greater than the height of the opening. (e.g., bottom slot in fig. 3):

$$D > a_i - y_i(t) \quad (6)$$

where  $D$  is the boulder's diameter,  $a_i$  is the height of opening number  $i$  and  $y_i(t)$  is the level of a lateral boulder jam at the base.

- *Combined jamming* occurs after sequential phases of lateral and/or vertical jamming (e.g., middle slot in fig. 3).

In order to numerically implement these jamming conditions, information about the number and size of boulders transported by a debris flow event and passing, at the same time, through a retention dam's openings should be computed. The first step is to define  $J$  classes of boulders assumed to be spherical on average. Each class  $j$  corresponds to a range of boulders' diameters  $[D_{j,min}, D_{j,max}]$  and is characterized by an average diameter  $D_j$  and a volume  $V_j$  estimated as follows:

$$D_j = \frac{1}{2}(D_{j,min} + D_{j,max}) \quad (7)$$

$$V_j = \pi D_j^3 / 6 \quad (8)$$

Moreover, in a given debris flow event of reference whose total volume is  $V_{ref}$ , one can count the actual number  $n_j$  of transported boulders of each class.  $V_{ref}$  should be large enough to be statistically representative, i.e., to assume that it provides a representative number of boulders of each class  $j$ . For each class  $j$ , the same volume  $V_{ref}$  can be split in  $N_j$  packets of elementary volumes  $V_j$  as represented in fig. 4. However, each of the obtained packets of debris can be either a boulder of class  $j$  or a boulder of another class or mud. Consequently, Piton et al. (2022) proposes to use a binomial law providing the number of successes  $n_j$  (i.e., actual boulder) in a sequence of  $N_j$  independent runs (i.e., number of packets) each of which yields success with probability  $p_j$ . The counting of the number of boulders per number of packets is used to calibrate  $p_j$  to later randomly compute which of the packets passing through an opening

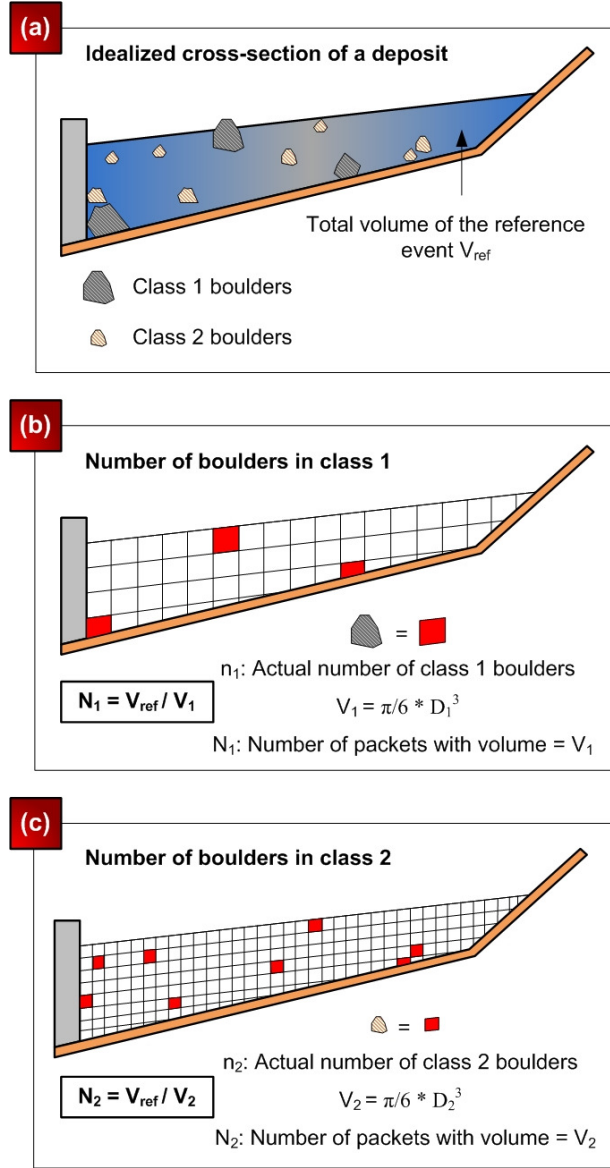


**Figure 4:** Conceptual schematic of boulder analysis used to calibrate the binomial distribution: (a) an idealized cross-section of a debris flow deposit with a given volume  $V_{ref}$  and a certain number of boulders belonging to two different size classes in a debris basin; (b) a more idealized version of the same deposit, where only the boulders of class 1 are represented: true boulders (red polygons) and false boulders (white polygons); (c) same concept but for boulders of class 2. Adapted from (Piton et al., 2022).

are actual boulders (success of the binomial law) and which are mud or boulders of other classes (failure of the binomial law). The success probability  $p_j$  of each class used in the binomial law is estimated using Eq. 9.

$$p_j = \frac{n_j}{N_j} = \frac{n_j}{V_{ref}/V_j} \quad (9)$$

Assuming that the frequencies of boulder classes are homogeneous on average across the entire flow,  $p_j$  can be adopted for any volume of a debris flow, interacting with an opening. Therefore, the number of boulders of each class  $n_j$  involved in a volume of debris flow  $V_i(t) = Q_i(t) \cdot \Delta t$  at a specific time can be obtained by simulating  $N_j = V_i(t)/V_j$  trials using a binomial distribution of parameter  $p_j$ . The time step  $\Delta t$  has been defined as 2 s in our case, with the

aim of both capturing the peak discharge and reducing computational time. The probability mass function  $P$  of the probability that  $n_j$  is exactly equal to a given value  $k$  is:

$$P(n_j = k) = \binom{N_j}{k} \cdot p^k \cdot (1 - p)^{N_j - k} \quad (10)$$

#### 2.2.4. Step 3: Buffering Capacity of a Debris Basin

Debris materials are stored in the debris basins and can be expected to escape gradually through the retention dam. The jamming of the dam's openings by boulders reduces their discharge capacities and thus the volume stored in the basin will significantly increase, which in turn reduces the buffering capacity of the basin during the event and subsequent ones. In such cases, the dam will no longer be able to self-clean a filled basin, which will have to be cleaned manually by carrying out maintenance operations.

Knowing the characteristics of the debris basin (storage capacity, deposition slope, stage-volume capacity curve) in addition to input hydrographs of debris flow events, the buffering of input flows in the basin can be estimated using the following mass conservation equation:

$$(Q_{inlet}(t) - Q_{outlet}(h(t))) \cdot \Delta t = \Delta V_b(h(t)) \quad (11)$$

where  $Q_{inlet}$  ( $m^3/s$ ) is the inlet discharge provided by the input hydrograph (fig. 2a),  $Q_{outlet}$  ( $m^3/s$ ) is the outlet discharge (Eq. 4),  $\Delta t$  ( $s$ ) is the time step,  $h$  ( $m$ ) is the flow level at the dam and  $\Delta V_b$  ( $m^3$ ) is the variation of the volume stored in the basin. The stored volume in the basin  $V_b$  for a specific flow level  $h$  can be extracted from the stage-volume capacity curve corresponding to the deposition slope (fig. 2a).

#### 2.2.5. Overall Computational Analysis

A code for solving all previous steps was written in R to model the time-dependent evolution of the volume stored in the debris basin. For a given structure, it first loads the structure features (fig. 2a): (i) retention dam geometry and (ii) debris basin stage-volume curve. It secondly loads the boulder counting for the reference volume (fig. 4) and computes the associated probability  $p_j$ . It then takes as an input the volumes of the debris flow events involved in a scenario. For each event, it goes through the following main steps:

- *Step 1* Defining an input vector that involves the volume of the debris flow event  $V_{event}$ , peak inlet discharge  $Q_{peak}$  based on Eq. (1), time to peak  $t_{peak}$ , deposition slope, initial volume stored in the basin  $V_{init}$  and initial lateral and vertical jamming rates of the dam's openings.
- *Step 2*: Building the inlet hydrograph of the event, which provides the inlet discharge  $Q_{inlet}(t)$ .
- *Step 3*: Estimating the initial level  $Z$  ( $m$ ) of deposit depending on the initial volume stored in the basin  $V_{init}$  ( $m^3$ ) using the stage  $h$  ( $m$ ) - volume  $V_b$  ( $m^3$ ) capacity curve.
- *Step 4*: Computing the outlet discharge  $Q_{outlet}$   $m^3/s$  through the retention dam using Eq. (4) taking into account only the initial lateral and vertical jamming rates of the dam's openings.
- *Step 5*: Randomly sampling the number of boulders of each class that approaches the openings of the dam using the binomial distribution approach presented in section 2.2.3.
- *Step 6*: Estimating the lateral and vertical jamming rates of the dam's openings based on jamming conditions (Eqs. 5 and 6) and updating the dimensions of the dam's openings.
- *Step 7*: Estimating the volume stored in the basin  $V_b$   $m^3$  using Eq. 11.

In order to model the evolution of indicators over time, steps 4 – 7 are performed at each time step over the whole duration of a debris flow event. The main outputs obtained after running the code are the time series of the inlet discharge  $Q_{inlet}(t)$  ( $m^3/s$ ), outlet discharge  $Q_{outlet}(t)$  ( $m^3/s$ ), lateral and horizontal jamming rates (%) of the dam's openings, flow level at the dam  $Z(t)$  (*m.a.s.l* - meters above sea level) and the cumulative volume stored in the basin  $V_b(t)$  ( $m^3$ ). Since the objective of the approach is to analyze the behavior of the retention dam over 50 years, the generated debris flow events involved within a scenario should be modeled one after another. In other words, the outputs provided after running event  $n$  in terms of filling state and jamming rates will be the initial inputs provided for analyzing event  $n + 1$ . This results in deterioration trajectories corresponding to the evolution of the indicators to be studied over time (e.g., volume stored in the basin).

### 2.3. Surrogate Stochastic Deterioration Model Implementing a CBM policy using SPNs

The developed scenario-driven physics-based model represents the physical process behind the filling of a debris basin over time. However, such a model is not really adapted for studying and assessing the performance of different possible maintenance policies (e.g., CBM) as it is a combination of several sub-models handled in sequence. Consequently, a surrogate stochastic deterioration model, which provides a simpler but comprehensive representation of the physical deterioration process capturing all its variability and uncertainty, should be developed in order to easily implement a CBM policy.

Several decision-support modeling tools exist and are widely used for modeling event-driven dynamic systems while combining deterioration, inspection and maintenance processes. Stochastic Petri nets SPNs (Signoret, 2009), stochastic activity networks SANs, (Sanders and Meyer, 2001), colored stochastic Petri nets CSPNs, (Zimmermann, 2008) and many other decision support tools could be used for this purpose. SPNs have already been adopted to model the deterioration and maintenance processes of complex structures and systems (Le et al., 2017; Yianni et al., 2017; Ferreira et al., 2018). It has also been recently adopted in the context of protection structures for optimizing maintenance strategies of torrent check dams (Chahrour et al., 2021). The latter revealed that SPN is an adequate tool that adapts to the current study's needs. Accordingly, a SPN model implementing a CBM policy is developed in this study in order to support maintenance decision-making of a debris basin subject to loss in capacity due to its filling by debris materials over time. All the processes involved in the SPN model are described in the following subsection.

#### 2.3.1. Physics-Informed Deterioration Process

The deterioration process of a SPN model is composed of four main elements: places, tokens, transitions and arcs (Petri, 1962). Places represent the states of the studied deteriorating system. These states correspond to different levels of deterioration of the system. The presence of a token in one of the places reveals that the system is residing in the state corresponding to this place. Stochastic transitions are responsible for moving the token from one place to another based on the probability laws assigned to the transitions. Arcs show the possible paths between the states of the system by linking between places and transitions. Consequently, in order to build a stochastic deterioration process of a debris basin using SPNs, two major steps should be achieved: (1) defining deterioration states of the basin and (2) learning probability laws corresponding to the transitions between the defined states.

The stochastic transitions are the key elements responsible for the functioning of the deterioration process. In most studies dedicated to complex system analysis, the probability laws associated with these transitions are either assumed based on expert assessment to follow probability distributions that are revealed to be adequate for modeling the deterioration process (e.g., Weibull, Poisson, Gamma) or are estimated based on real data concerning time to failure (Le et al., 2017; Yang and Frangopol, 2019; Tao et al., 2021). Such kind of assumptions could only be a limitation when real data about undesirable events, failure modes and failure rates are missing, which is the case for protection systems in mountains. For this purpose, scenario-driven physics-based models are first developed in order to describe the physical mechanisms underlying the deterioration process, also accounting for the associated variability and uncertainty. The outputs of these physics-based models are then used to learn the stochastic transition laws between the states of the system.

As previously mentioned, the volume stored in the debris basin is chosen as the major deterioration indicator in this study. However, the physical modeling of this indicator already incorporates other deterioration indicators such as the jamming rate of the retention dam's openings. Using the framework presented in section 2.2.5, the modeler can start the modeling considering an empty basin and then assess how the retention system moderates (buffer) debris flow events over time. Indeed, the stored volume in a basin  $V_b$  can evolve progressively or rapidly from an initial state (e.g., empty basin) to deteriorated states (e.g., partially filled basin) until reaching a completely failed state (e.g., completely filled basin). In the present study, four different states of filling that reflect the condition of the debris basin are defined: good, poor, very poor and failed conditions. The thresholds corresponding to the intervals that define these states are determined based on expert judgment and could, of course, be discussed and modified. The states and their associated intervals are described below:

**State 1:** good condition with  $0 \leq V_b < V_{P1}$

**State 2:** poor condition with  $V_{P1} \leq V_b < V_{P2}$

**State 3:** very poor condition with  $V_{P2} \leq V_b < V_{P3}$

**State 4:** failed condition with  $V_{P3} \leq V_b \leq C_b$

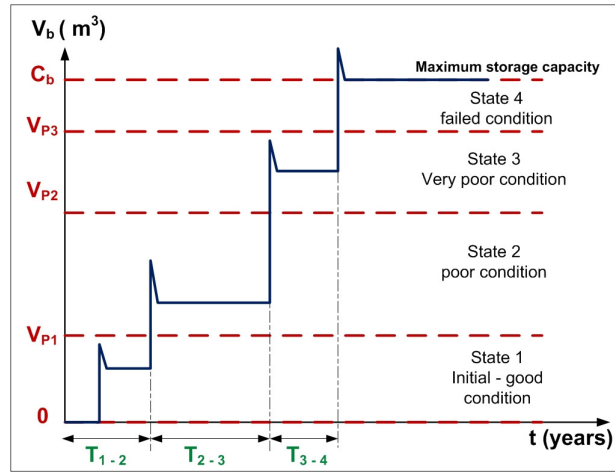


**Figure 5:** Example showing the evolution of the debris volume stored in the basin  $V_b$  over time.

where 0 corresponds to an empty basin.  $V_{P1}$ ,  $V_{P2}$ , and  $V_{P3}$  are the states' indicator thresholds.  $C_b$  is the maximum storage capacity of the basin.

The physical modeling presented in section 2.2 provides observations of a debris basin's stochastic deterioration trajectories. The number of observations depends on the number of considered debris flow scenarios. Based on these trajectories, several realizations of the random transition times between the defined states can be obtained, based on which it is possible to learn the transition laws by estimating a non-parametric cumulative distribution function for each transition (Kaplan and Meier, 1958). Fig. 5 provides an example of one random deterioration trajectory showing how  $V_b$  evolves from one state to another over time in the case where no maintenance operations are carried out. It is important to differentiate between the maximum volume stored in the basin attained during each event and that attained at the end of the event. In fact, the maximum stored volume is usually higher than the final stored volume due to self-cleaning. However, the volume stored at the end is the most important for the maintenance aspect.

The deterioration process involved in the overall SPN model is represented in fig. 6a. The four states of the debris basin are represented by places  $P_1 - P_4$  corresponding respectively to the good, poor, very poor and failed conditions. The model is executed assuming that the basin is initially in good condition. This explains the presence of a token (small solid circle) in  $P_1$  at  $t = 0$ . The stochastic transitions responsible for the movement of the token from one place to another are represented as  $T_{x-y}$ , where  $x$  and  $y$  are the states at time  $t$  and  $t + 1$  respectively. Therefore, they reflect the evolution of the basin from one state to another. For example,  $T_{1-2}$  links between states 1 and 2 and  $T_{2-4}$  links between states 2 and 4. It is therefore important to note that the deterioration is not necessarily gradual. For example, the system can move from state 1 to either state 2, 3 or 4 depending on which of the transitions  $T_{1-2}$ ,  $T_{1-3}$  and  $T_{1-4}$  fires first. Usually, the transitions function based on a firing delay time associated with each transition. In other words, once all the transition conditions are verified, a transition is fired when its firing delay time is reached. Upon its firing, the token moves from the input place of the transition to its output place. For stochastic transitions, the firing delay times are drawn from probability distributions learned from the physics-based model as explained above.

The next step consists in modeling the evolution of the debris basin from one state to another when subjected to a CBM policy through a stochastic inspection and maintenance processes using SPNs.

### 2.3.2. Inspection and Maintenance Processes

Field visits should be carried out regularly in order to detect the state of the debris basin at a specific time. Several scenarios could be adopted concerning inspection times. For example, one scenario could be that each time an event happens, inspectors should go to the field, identify the level of deterioration and decide whether a maintenance operation is necessary or not. Another scenario could be that regardless of the level of deterioration attained during the year, a maintenance operation should be performed once a year. However, because of the yearly budget, harsh weather and difficulty in accessing the field, another scenario could be that inspectors are supposed to visit the field one time per year, consider the state of the basin and then to decide whether or not to apply maintenance. In other words, it is

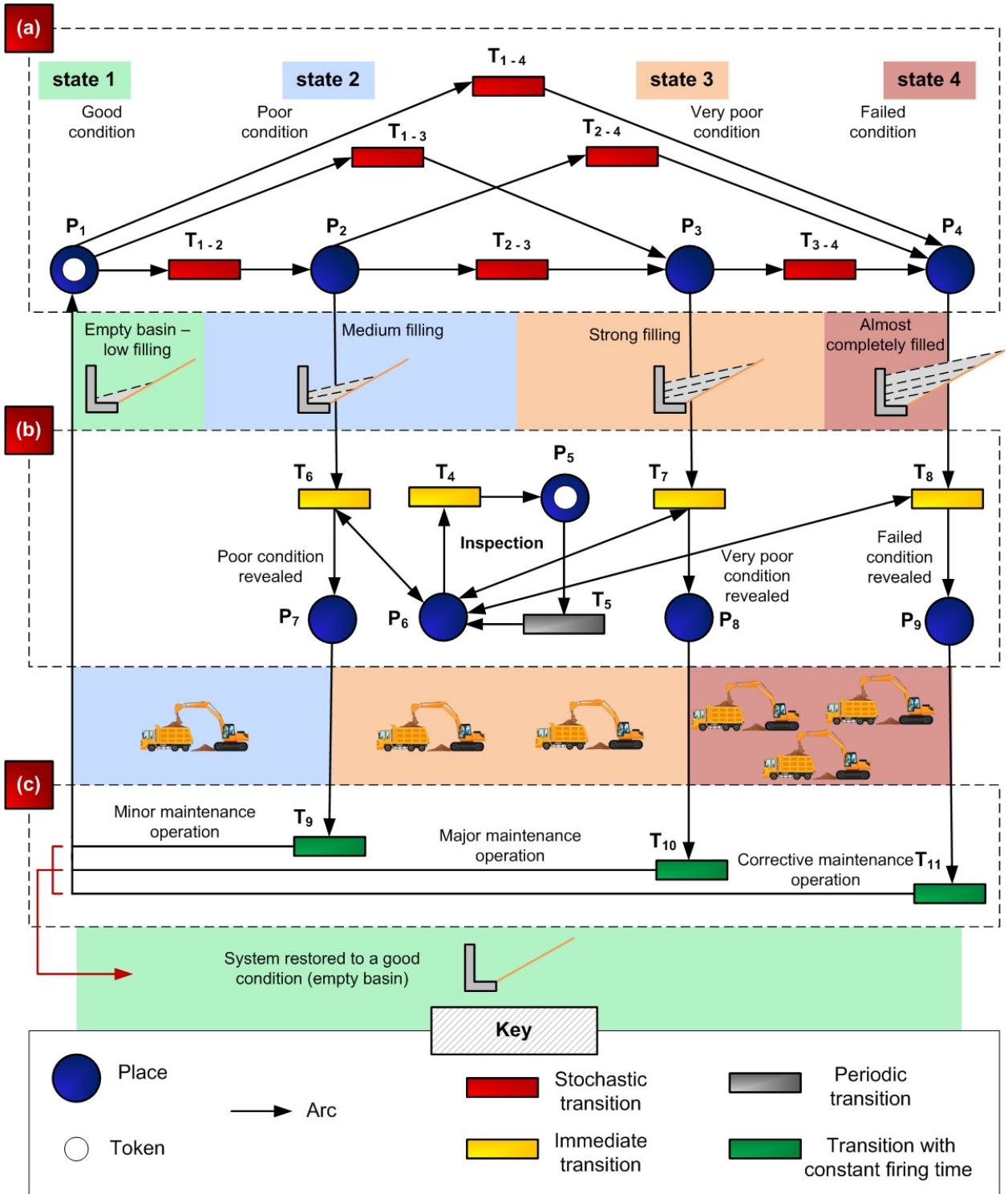


**Figure 6:** SPN model developed for modeling stochastic deterioration and maintenance processes of a capacity deteriorating debris basin. (a) Deterioration process; (b) inspection process and (c) maintenance process.

not necessary that they will take the decision to do maintenance upon inspection. The latter scenario is the one adopted

in this study, in which inspection is scheduled once per year and thus decision whether to apply maintenance or not is only made once per year.

Fig. 6b represents the inspection process of the developed SPN model. Initially, a token is present in place  $P_5$ , which is linked to the periodic inspection transition  $T_5$ . Consequently, after one year  $T_5$  is fired and the token in  $P_5$  moves to  $P_6$  at which inspection takes place. Depending on the state of the basin detected upon inspection, one of the immediate transitions  $T_6$ ,  $T_7$  or  $T_8$  will immediately fire and a token will be present respectively either in place  $P_7$ ,  $P_8$  or  $P_9$ . The bi-directional arcs connecting  $T_6$ ,  $T_7$  and  $T_8$  with  $P_6$  make  $P_6$  both an input and an output place for these transitions. Therefore, when any of these transitions fires, it retrieves tokens from its input places while depositing one token into its output place, which is  $P_6$ . Thus, even after the firing of  $T_6$ ,  $T_7$  or  $T_8$ , a token remains in  $P_6$ . In order for an inspection to be scheduled again,  $T_4$  also fires immediately so that the token in  $P_6$  returns to  $P_5$  waiting for the next inspection after one year. To prevent conflicts between the firing of  $T_4$  and  $T_6$ ,  $T_7$  or  $T_8$ , it's necessary to assign priorities to these transitions. Consequently, a lower priority is assigned to  $T_4$  to ensure that  $T_6$ ,  $T_7$  or  $T_8$  fires first.

Each year the state of the basin is monitored once. Following this monitoring inspection, a specific maintenance plan depending on the level of deterioration should be scheduled. This corresponds to a CBM policy associated with a discrete deterioration process. Several CBM policies can be adopted for the developed deterioration process. In this study, the chosen policy is represented by fig. 6c. After inspection, if there is no token in  $P_7$  nor in  $P_8$  nor in  $P_9$ , the basin is revealed to be residing in state 1 and no maintenance operation is scheduled. If a token is present in  $P_7$ ,  $P_8$  or in  $P_9$ , a minor, major or corrective maintenance operation should be applied respectively. Each maintenance operation has a constant firing time corresponding to the time needed for the operation to be carried out. After this time, transition  $T_9$ ,  $T_{10}$  or  $T_{11}$  fires and a token is placed again in place  $P_1$  which corresponds to state 1 in the deterioration process. This reveals that the maintenance operations are assumed to be perfect, in which they restore the basin back to its initial state.

It is necessary to highlight here the fact that it is possible for the basin to deteriorate from one state to another prior to inspection. This means that the basin is not necessarily maintained when it reaches a state where a maintenance operation is required. For example, if the basin is in state 2, there exist three possible pathways: (1) if transition  $T_6$  fires first, meaning that inspection took place, the token present in  $P_2$  moves to  $P_7$  and a minor maintenance operation will be carried out; (2) if transition  $T_{2-3}$  fires first, the token in  $P_2$  moves to  $P_3$  meaning that the system has deteriorated to state 3 before applying maintenance and (e.g., another debris flow events occurred and partially filled the basin) (3) if transition  $T_{2-4}$  fires first the token in  $P_2$  moves to  $P_4$  revealing that the system has deteriorated directly to state 4 before any inspection (e.g., another debris flow events occurred and rapidly filled the basin).

### 2.3.3. SPNs as Model-Based Decision Support Systems

The flexibility of SPNs makes it possible to use the same structure presented in fig. 6 but assign different functionalities. Because the end purpose of this study is to support maintenance decision-making of a debris basin in a retention system, four different maintenance strategies can be considered for comparison within the SPN model:

*Strategy 1:* all maintenance operations are allowed. The basin can be maintained when it reaches states 2, 3 or 4.

*Strategy 2:* minor maintenance operations are inhibited. The basin is allowed to deteriorate further than state 2 without any maintenance operation.

*Strategy 3:* Major maintenance operations are inhibited. When the basin reaches state 3, it is allowed to deteriorate further to state 4 without any maintenance operation.

*Strategy 4:* only corrective maintenance operations are allowed. The basin is only maintained when it reaches a completely failed state.

In order to compare the proposed maintenance strategies, each strategy is simulated separately. Indeed, after Monte-Carlo simulations, the SPN model provides for each maintenance strategy two major outputs: (1) the mean time spent by the basin in each of the defined states and (2) the mean number of maintenance operations performed over the specified period of simulation. These outputs make it possible to sort maintenance strategies in terms of cost (depending on the cost of each operation) and maximum availability (time spent in a non-failed state). This in turn supports risk managers to make suitable maintenance decisions depending on the efficiency of the maintenance strategy in increasing the level of protection provided by the retention system and on available budgetary resources.

### 3. Case Study: Claret's Retention System

This section presents a brief description of the case study to be considered in this paper. It starts by introducing the Claret torrent, the features (type, frequency) of the torrential events that occurred in the torrent in addition to the retention system implemented in this torrent. The section also presents the acquired, estimated and generated data necessary for the deterioration modeling and maintenance optimization that will be tackled in the next section.

#### 3.1. General Description of the Claret Torrent and its Debris Retention System

The Claret torrent is a tributary on the right bank of the Arc River whose confluence is in the town of Saint Julien Montdenis in the Maurienne valley (Savoie) in France. It is a very active torrent characterized by a steep slope and high sediment potential. According to the event's history, this torrent has a frequent tendency to produce muddy debris flows. These events can contain a significant volume of materials and can carry large boulders sometimes up to its confluence with the Arc. Historical archives of torrential events show that floods occur with a very high frequency during intense summer storms (up to three events per year), with an average frequency of five significant debris flow events per decade (Hugerot, 2015). All recorded damaging events have almost caused the same damages such as bridge collapsing, roads and railways blockage by large boulders and alluvial fan incision. Protection structures such as check dams were built in 1957 in order to stop torrential floods, reduce their intensities and stabilize the longitudinal profile. Nonetheless, a violent debris flow event occurred on July 2, 1987 and caused severe damage to exposed issues located in downstream due to the transfer of very large boulders. This debris flow is considered as a reference event that urged risk managers to implement a debris retention system to protect downstream exposed assets (EDF channel, roads, railway) from the very large boulders that contribute to the geomorphic activity of the torrent.

Indeed, in 1991, a debris retention system was built in the Claret torrent. The objective was to store large boulders transported by debris flow events in the debris basin and to moderate the passage of the flow through the openings of the dam. The debris basin is 120 m long with a capacity of 22,000 m<sup>3</sup>. It is closed by a 9.2 m high reinforced concrete retention dam. The dam has three openings: two separate rectangular slots and a trapezoidal spillway as shown in fig. 1. The main objectives of the bottom slot are to allow low-magnitude events to pass through the dam towards the downstream and to stop boulders with diameters greater than 1 m. The middle slot is only activated when the deposit level upstream of the dam reaches 4 m of debris. Moreover, the trapezoidal spillway directs extreme flows over the dam when the deposit is more than 7 m high. Since its construction, the dam has stored excessive volumes of debris even those carried by low-magnitude debris flows, which could have passed smoothly to downstream. Consequently, the dam's lower opening is not sufficient in relation to the maximum diameter of the boulders, which are transported during frequent debris flows. This issue necessitates regular cleaning operations in order to remove the stored materials in the debris basin and thus ensure the functional efficacy of the retention system. This in turn has requested high monetary budgets.

Managers of the Claret used to adopt a specific maintenance policy. Each time a debris flow occurs, they ask for scheduling maintenance where all the stored volume should be cleaned. In this study, the aim is to explore alternative maintenance policies. Instead of event-based maintenance, condition-based maintenance is adopted in which cleaning maintenance decision depends on the state of the basin detected after inspection. This is achieved by modeling the progressive filling of the Claret's debris basin considering the jamming rate of the dam's openings when subjected to debris flows over a period of 50 years.

#### 3.2. Numerical Modeling Inputs and Data Sources

Prior to modeling and analysis, several numerical inputs should be acquired. This section presents the data necessary for executing simulations using the approach developed in section 2.

##### 3.2.1. Random Debris Flow Scenarios

Data concerning the average number of torrential floods that occur during every month of the year is extracted from the database of the system's managers (ONF-RTM, i.e., French torrent control service). Fig. 7 shows the monthly distribution of all recorded floods in the Claret and the corresponding cumulative distribution function CDF (ONF-RTM, 2013). It can be noticed that almost all of the events (87 %) occur between June and September due to summer rainstorms, which are often very intense.

Morel et al. (2022) gathered data concerning the volumes of past events recorded from 1992 until 2019, which enabled to fit a generalized Pareto distribution (GPD) to build a "Frequency - Magnitude" curve of the Claret catchment on an observation period of barely 27 years (fig. 8). The GPD adjustment is characterized by a shape parameter

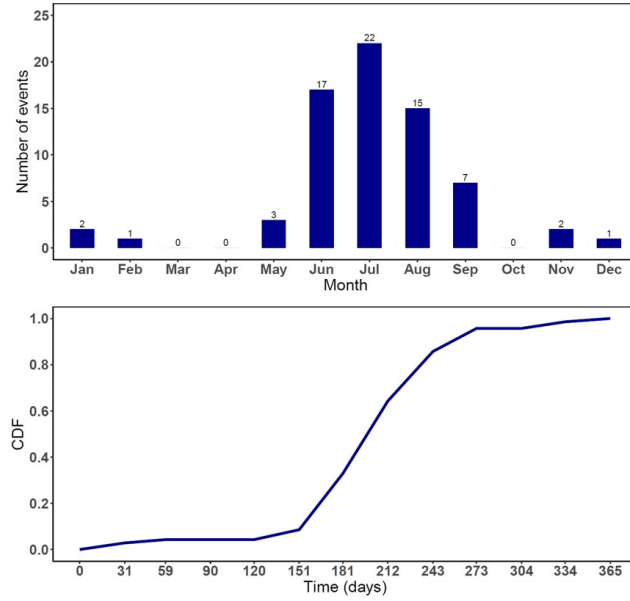


**Figure 7:** Histogram and CDF corresponding to the monthly distribution of recorded torrential floods in the Claret. Data extracted from (ONF-RTM, 2013).

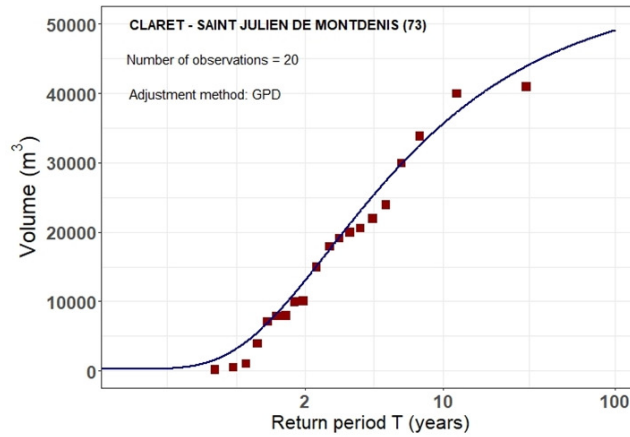


**Figure 8:** Claret's Frequency - Magnitude curve resulted after the adjustment of real observations of debris flow events using GPD distribution. Adapted from (Morel et al., 2022).

( $\xi = -0.49$ ) and a scale parameter ( $\beta = 27,172.8$ ). This probabilistic law will be used to randomly sample debris flow event scenarios based on real observations. It also makes it possible to compute the volume of debris flows with given return periods. For example, the volumes corresponding to return periods of 10, 20, 50 and 100 years are respectively 35,500, 41,000, 46,000 and 49,000  $m^3$ .

In order to achieve the desired objective of this study, 100 debris flow scenarios that involve debris flows occurring over a period of 50 years are generated. For each scenario, based on archives, it is considered that three storms sufficiently intense to eventually trigger a debris flow occur per year. However, not all of these storms lead to debris flows, often due to a lack of available transportable materials. This implies that a total of  $N = 150$  storms are randomly sampled over the studied period. To figure out whether each of the three events triggers a debris flow, a binomial distribution is again adopted. Since on average, one debris flow occurs every two years, it is expected to have one debris flow event every six storms on average. Therefore, the success probability used in the binomial law is  $p = \frac{1}{6}$ .

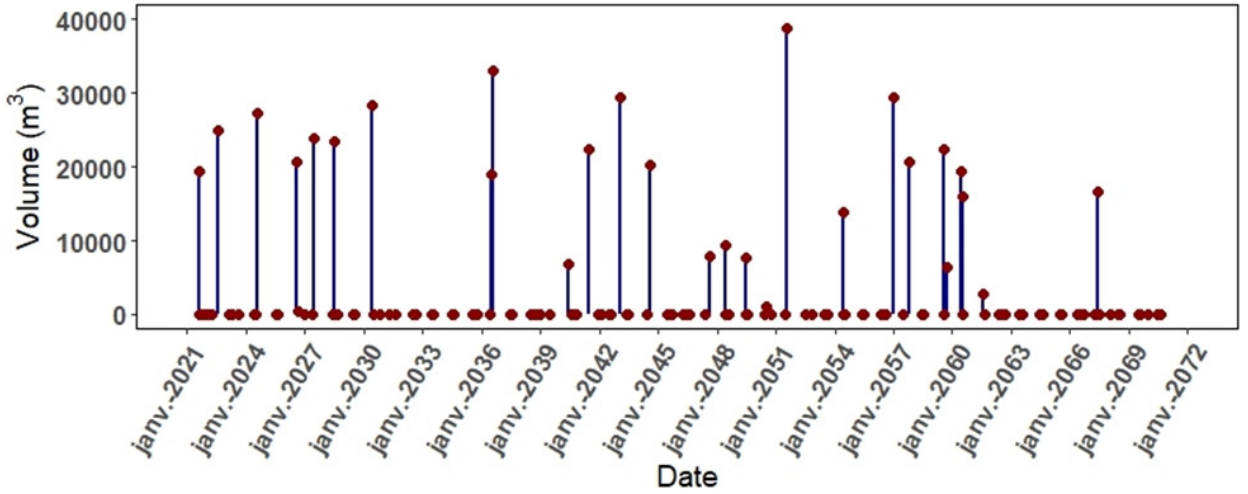


Figure 9: Time series of torrential floods and triggered debris flow events over a period of 50 years - Scenario 1.

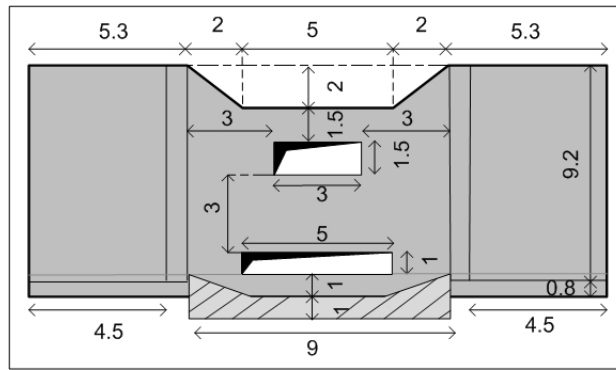


Figure 10: Claret's retention dam's detailed geometry and dimensions (in  $m$ ) - Front view.

In the case when a debris flow is triggered, a random volume is picked up from the GPD fitting of fig. 8. Otherwise, the debris flow volume is set to  $0 m^3$ .

With regards to the dates of occurrences of the 150 storm events involved in each scenario, 150 dates are randomly sampled from the CDF that belongs to the real empirical data presented in fig. 7. All generated dates are then sorted in ascending order and associated with the 150 generated volumes. Fig. 9 shows the time series of events corresponding to the first generated scenario (scenario 1). The hydrographs are assumed to have a triangular shape with a peak discharge attained after 5 s of the event's starting time based on the monitoring observations of Piton et al. (2018).

### 3.2.2. Initial Configuration of the Retention System

Fig. 10 provides a detailed illustration of the geometry of Claret's retention dam. All related information concerning the dam's openings is provided in table 1. Both, the two rectangular slots and the trapezoidal spillway are assumed to be initially empty from boulders (jamming rate = 0%). In order to estimate the number of boulders that could be transported by a given debris flow volume and could interact with the dam's openings, data concerning the class and the number of boulders observed in a reference volume of  $V_{ref} = 30,000 m^3$  were predicted by expert judgement and presented in table 2.

One more necessary piece of information concerns the deposition slope in the debris basin. The actual deposition slope was measured as  $S_{dep} = 6.1 \%$  on the topographic data collected after the 2017 debris flow (Piton et al., 2018). Another topographic survey of the basin state before its filling made it possible to build for the estimated  $S_{dep}$ , the stage  $h$  (m.a.s.l) - volume  $V_b$  ( $m^3$ ) capacity curve using 3D analysis. Initially, before the first event involved in each

**Table 1**

Characteristics of the Clarte's retention dam's openings.

Number	Type	Width (m)	Base level (m.a.s.l)	Top level (m.a.s.l)	Inclination angle with horizontal (°)
1	Bottom slot	5	690	691	-
2	Middle slot	3	694	695.5	-
3	Spillway	5	697	-	45

**Table 2**Number of boulders with different diameters that can be found in a reference volume of 30,000 m<sup>3</sup>.

Diameter (m)	Number
3	2
2	10
1	200

scenario, the debris basin is considered to be empty of materials ( $V_b(t=0) = 0 \text{ m}^3$ ) and the initial level of deposits at the retention dam is  $Z(t=0) = 690 \text{ m.a.s.l.}$

The volume stored in the basin  $V_b$  evolves during each debris flow event. As mentioned in section 2.3.1, the basin can reside in four different states defined depending on the value of  $V_b$ . Based on experts' judgment, the thresholds of these states are chosen as follows:

**State 1:** until 10% of the basin's capacity

$$0 \text{ m}^3 \leq V_b < 2,200 \text{ m}^3$$

**State 2:** before reaching about half the basin's capacity

$$2,200 \text{ m}^3 \leq V_b < 10,000 \text{ m}^3$$

**State 3:** before reaching 90% of the basin's capacity

$$10,000 \text{ m}^3 \leq V_b < 20,000 \text{ m}^3$$

**State 4:** until the basin is 90% filled

$$20,000 \text{ m}^3 \leq V_b \leq 22,000 \text{ m}^3$$

### 3.2.3. SPN Model Inputs and Economic Data

The SPN model presented in fig. 6 will be used to study the stochastic evolution of the debris volume stored in Claret's debris basin while carrying out CBM operations. Minor, major and corrective maintenance operations corresponding respectively to states 2, 3, and 4 are defined. Usually, for the case of maintaining debris basins, the same maintenance policy is carried out whatever the state of the basin is. In other words, after inspection, whatever the state of the filling is, the decision is to clean all the volume stored in the basin. The difference in minor, major and corrective operations lies only in the amount of materials to be cleaned and therefore the duration required to carry out each operation.

The deterministic transition times of fig. 6, corresponding to the inspection frequency ( $T_5$ ) in addition to the time required to schedule and achieve each maintenance operation ( $T_9$ ,  $T_{10}$  and  $T_{11}$ ), are assessed by experts and presented in table 3. The time required for carrying out cleaning operations ranges between 3 to 12 months (Paulhe et al., 2018). In June 14<sup>th</sup> 2017, a debris flow with  $V_b \approx 8000 \text{ m}^3$  (a typical State 2 maintenance) occurred. The cleaning maintenance operation took about one month (Sept. 3<sup>rd</sup> - Oct. 11<sup>th</sup>) but it was launched 2.5 months after the event (scheduling time). Consequently, it is assumed that the launching time is fixed to 2.5 months and the cleaning period is proportional to the volume to be cleaned. The constant firing times corresponding to transitions  $T_9$ ,  $T_{10}$  and  $T_{11}$  are therefore estimated as follows:

- *Minor operations:* 2.5 months + 1 month for state 2
- *Major operations:* 2.5 months + 2 months for state 3

**Table 3**

Deterministic transition times involved in the inspection and maintenance processes involved in the SPN model.

Process	Transition	Constant firing time (years)
Inspection	$T_5$	1
	$T_4 T_6 T_7 T_8$	0
Maintenance	$T_9$	0.291
	$T_{10}$	0.375
	$T_{11}$	0.458

**Table 4**

Costs of maintenance operations carried out for cleaning Claret's debris basin.

Operation	Mean cleaned volume ( $m^3$ )	Cost (€)
1	6,100	17,000
2	15,000	42,000
3	21,000	59,000

- *Corrective operation*: 2.5 months + 3 months for state 4

Since the implementation of Claret's retention system, the average cost of cleaning operations has been  $2.83 \text{ €/m}^3$  (Paulhe et al., 2018). It is assumed that the average volume of the interval defining the states at which the maintenance operations are required is considered for estimating the cost of each operation. These costs are presented in table 4 and are consistent with the variation of cleaning costs presented in the literature (Carladous et al., 2022).

## 4. Results and Discussions

This section presents the results provided after modeling the deterioration and maintenance processes of the Claret retention system when subjected to the 100 generated debris flow scenarios over a period of 50 years.

### 4.1. Deterioration Trajectories of the Claret's Debris Basin

The 100 generated debris flow scenarios are simulated using the scenario-driven physics-based model developed in section 2.2. Fig. 11 exemplifies its results with the first two consecutive debris flow events involved in scenario 1 (event 1:  $V_{event} = 19,422 \text{ m}^3$ ,  $D_{event}$ : 14/08/2021 ; event 2:  $V_{event} = 24,873 \text{ m}^3$ ,  $D_{event}$ : 07/08/2022 ). During the first event, the retention system trapped  $9,300 \text{ m}^3$ , i.e., decreased the volume of the debris flow by 52% and released the un-trapped material with a peak discharge of  $27 \text{ m}^3/\text{s}$ , i.e., buffered the peak discharge by 42%. During the second event, the higher jamming of the dam's slots (totally black lines in second and third panels of fig. 11b) lead to higher trapping of  $12600 \text{ m}^3$ , i.e., 49% of the supply, as well as a higher buffering of 70%, releasing a maximum discharge of  $17 \text{ m}^3/\text{s}$  against  $55.8 \text{ m}^3/\text{s}$  at the inlet of the basin. It can also be noticed that during the second event, the flow level at the dam exceeded the spillway's level (dotted line in the fourth panel of fig. 11b). The final volume stored in the basin attained after the second event is  $V_b = 21,900 \text{ m}^3$ , which is approximately equal to the maximum storage capacity of the basin  $C_b = 22,000 \text{ m}^3$ . Both debris flows have reached their maximum deposition in less than 12 minutes and then have progressively self-cleaned a specific volume through the middle slot. At the end of event 2, the bottom and the middle slots of the dam were totally horizontally and vertically jammed by boulders (totally black first and second lines in the second and the third panels of fig. 11b).

Similar outcomes are obtained for other events and scenarios. Note that in addition to the stochastic model developed for generating random events, stochasticity is also present in another stage of the physics-based model, in which the presence and transport of boulders in a given debris flow volume are modeled using the binomial law (recall section 2.2.3). Consequently, results obtained after the simulation of a specific event differ when simulating again the same event due to the randomness in the number of boulders passing and jamming the dam's openings.

These outputs enable the modeling of the evolution of the volume stored in the debris basin  $V_b$  (deterioration indicator) taking into account dependencies with the jamming rate of the dam's openings (sub deterioration indicator).

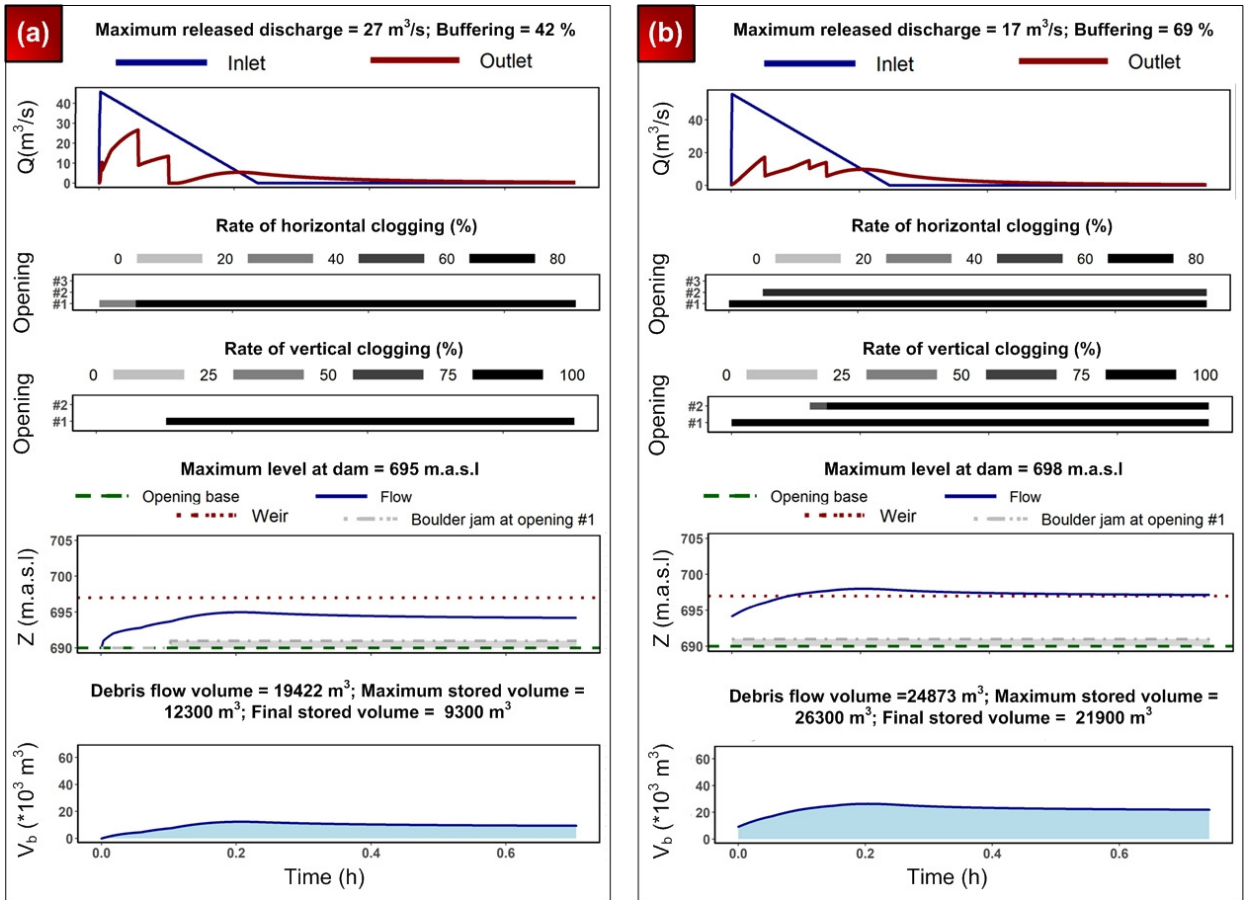


**Figure 11:** Results obtained from the buffering model involved within the physics-based model showing the variation of several physical parameters: (a) event 1 in scenario 1 and (b) event 2 in scenario 1.  $Q$  (m<sup>3</sup>/s) is the discharge,  $Z$  (m.a.s.l) is the flow level at the dam and  $V_b$  (\*10<sup>3</sup> m<sup>3</sup>) is the volume stored in the basin.

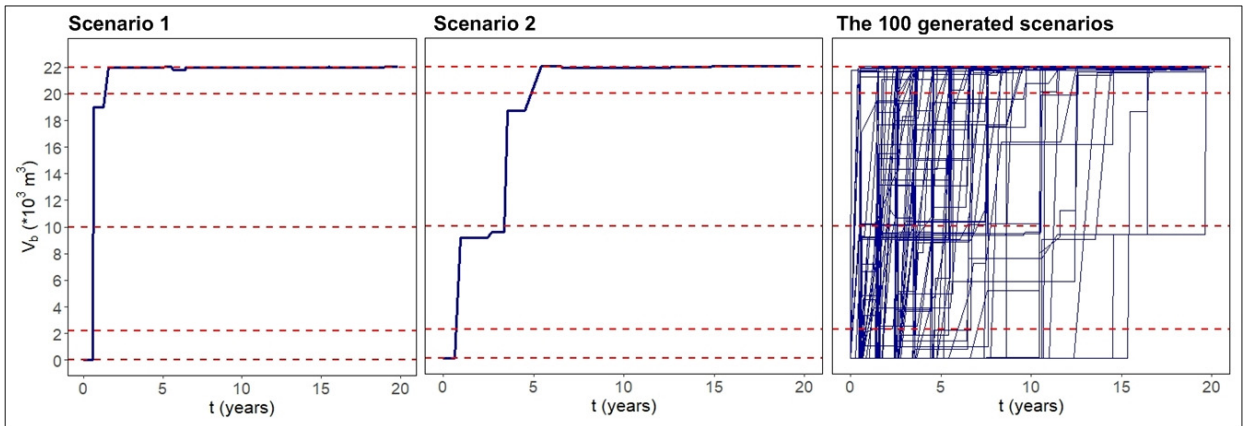


**Figure 12:** Time-dependent evolution of the state indicator  $V_b$  for the 100 generated scenarios. Blue curve: indicator evolution over time; red dashed lines: indicator thresholds (0 m<sup>3</sup>,  $V_{P1} = 2,200$  m<sup>3</sup>,  $V_{P2} = 10,000$  m<sup>3</sup>,  $V_{P3} = 20,000$  m<sup>3</sup> and  $C_b = 22,000$  m<sup>3</sup>).

Fig. 12, shows the time-dependent evolution of  $V_b$  for all of the 100 generated scenarios. The scattering seen in the

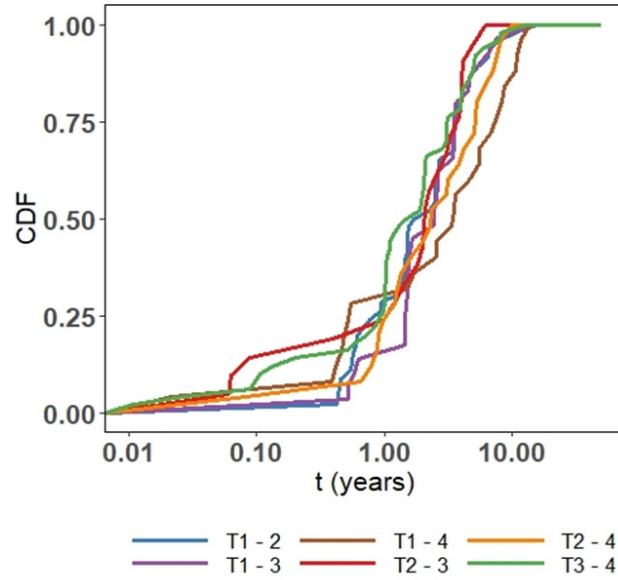


**Figure 13:** Cumulative distribution functions of the stochastic transitions involved in the deterioration process of the SPN model (logarithmic scale).

figure reveals that the evolution of  $V_b$  varies depending on the generated scenario. The variation is mainly controlled by the magnitude of the events involved in each scenario, and at the second order by the numbers and classes of boulders interacting with the dam's openings. This, again, proves the necessity of stochastic modeling in order to integrate possible behaviors of the system in the analysis. The basin is completely filled within 5 years in most scenarios and within 20 years in all scenarios. Therefore, maintenance is required at very early stages.

Estimating the time spent in each of the defined states for all the simulated scenarios provides a data set for each of the stochastic transitions that link between the states of the basin. From the obtained results, it is revealed that all transitions have a considerable number of observations, in which  $T_{1-2}$ ,  $T_{1-3}$ ,  $T_{1-4}$ ,  $T_{2-3}$ ,  $T_{2-4}$  and  $T_{3-4}$  have attained, respectively, 46, 29, 25, 21, 25 and 50 values out of 100 values. An empirical cumulative distribution function (CDF) is estimated for each transition using Kaplan-Meier estimator (fig. 13).

## 4.2. Maintenance Decision-Making

In order to support decision-making concerning cleaning maintenance operations, the obtained CDFs are used as an input to the deterioration process involved in the SPN model developed in section 2.3. Each CDF is assigned to its corresponding stochastic transition in fig. 6. The CDFs are represented by a two-dimensional matrix (delay, cumulative probability) so that the firing delay time of each transition can be estimated. In addition, in order to avoid conflict between transitions that have a common input place (e.g.,  $T_{1-2}$ ,  $T_{1-3}$  and  $T_{1-4}$ ), a firing probability is assigned to each transition based on its attained number of observations.

Since the SPN model follows a stochastic process, the number of simulations to be held is considered to be sufficient when the results stabilize and converge, signifying consistency in the outcomes. In this particular study, a total of 1000 Monte-Carlo simulations were executed and convergence in results consistently occurred after just 200 simulations for all predefined maintenance strategies. Tables 5 and 6 summarize the results obtained for each maintenance strategy modeled over a period of 50 years.

Table 5 reveals the influence of each maintenance strategy on the mean sojourn time of the Claret's debris basin in the four defined states. In strategies 1 and 3, the basin resides in state 1 for a longer period of time when compared to strategies 2 and 4. This is due to the fact that in strategies 1 and 3, maintenance is applied as soon as the basin is no more in good condition using minor operations. On the other hand, for strategies 2 and 4, where minor maintenance is prevented, the basin remains in a poor condition (state 2) for a longer time. In strategy 3, since major maintenance is inhibited, the basin resides in a very poor condition (state 3) for a long time in comparison to the strategies where

**Table 5**

Mean sojourn time (years) of the Claret's debris basin in each of the defined states depending on the adopted maintenance strategy.

Strategy	State 1	State 2	State 3	State 4
1	40.49	3.36	2.67	3.48
2	31.05	10.94	3.19	4.82
3	33.55	2.93	7.77	5.74
4	25.32	9.42	8.19	7.07

**Table 6**

Statistics on the number of cleaning maintenance operations performed over a period of 50 years depending on the adopted maintenance strategy.  $\mu$ : average;  $\sigma$ : standard deviation.

Strategy	Minor		Major		Corrective	
	$\mu$	$\sigma$	$\mu$	$\sigma$	$\mu$	$\sigma$
1	4.84	2.15	3.66	1.87	4.14	1.64
2	0.00	0.00	4.09	1.75	5.29	1.65
3	4.09	2.16	0.00	0.00	6.44	1.71
4	0.00	0.00	0.00	0.00	7.48	1.70

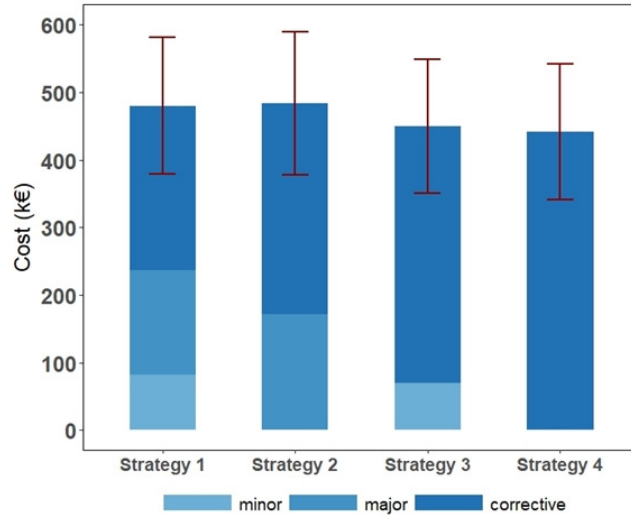
major operations are allowed (strategies 1 and 2). Concerning strategy 4 where only corrective operations are allowed, the basin spends more time in the deteriorated states 2 and 3 compared to other strategies. The reason behind this is that the basin continues to deteriorate without being cleaned until it completely fails by reaching almost its maximum storage capacity.

Table 6 shows that almost in all the proposed maintenance strategies, corrective maintenance operations, which are applied when the volume stored in the basin exceeds 90% of the basin's capacity are the most performed. This reveals that the basin reaches almost its storage maximum capacity within a short duration compared to the time at which the inspection is carried out. This issue can also be noticed in fig. 12, at which it is clear that the deterioration rate corresponding to the filling of the basin is very high in most of the scenarios (e.g., scenario 1).

#### 4.2.1. Optimization of Maintenance Costs

The statistics on the number of applied maintenance operations provided in table 6 make it possible to compute the total average cost of each of the proposed maintenance strategies. Indeed, the results provided in fig. 14 make it easy to sort, compare and choose the most cost-effective maintenance strategy. The cost represented in the figure is equal to the average of the 200 costs obtained from the 200 Monte-Carlo simulations of the SPN model. The figure also shows error bars, which represent the variability of the data provided by the 200 simulations. These error bars are edged lines that extend from the center of the plotted data (mean  $\mu$ ) according to the obtained standard deviation  $\sigma$ . In other words, the upper and the lower edges of the error bars correspond respectively to  $\mu + \sigma$  and  $\mu - \sigma$ . It can be noticed that all of the defined maintenance strategies have more or less the same total average cost. This can also be seen from the error bars which almost overlap, revealing that the difference between the four strategies is not statistically significant.

Regardless that the costs of all strategies are not so different, strategy 4 is revealed to be slightly cheaper than the other. In other words, waiting until the basin is more than 90% filled ( $V_b \geq 20,000 \text{ m}^3$ ) and cleaning the whole volume of deposits seems to be the most cost-effective strategy when considering only the cleaning of the basin (see next section). Strategy 2, where cleaning operations are applied when the basin is filled by more than 50% is the most expensive. Firstly, strategy 2 prevents minor cleaning operations that are typically performed during the early stages of basin filling, when it's less than 50% filled. This leads to an accumulation of debris materials without periodic maintenance, contributing to a higher cost compared to strategies 1 and 3 where minor operations are allowed. Secondly, strategy 2 requires cleaning operations when the basin reaches approximately 50% of its capacity, which results in significantly more material to remove during each cleaning operation. This increase in volume demands more workers, machinery and resources, ultimately driving up the cost. Compared to strategy 4, where cleaning occurs only at state 4, strategy 2 adopts a more proactive approach by cleaning at state 3 or 4. However, it's important to note that it takes the basin longer to reach state 4 than state 3. Consequently, strategy 4 involves fewer maintenance



**Figure 14:** Average total cost of the four proposed maintenance strategies. The error bars (in red) reveal the uncertainty around the average total cost (lower edge:  $\mu - \sigma$  and upper edge:  $\mu + \sigma$ ).

operations ( $\approx 7$  corrective operations), while strategy 2 necessitates more frequent cleaning ( $\approx 4$  major and 5 corrective operations). As a result, the implementation of strategy 2 results in more frequent cleaning operations, driving up the associated costs.

The scenario-driven physics-based model reinforces these interpretations, demonstrating that the debris basin is rapidly filled by debris materials, especially when the bottom outlet is jammed. Interestingly, and quite counter-intuitively, it is slightly cheaper to come more often, each time a deposit occurs. This is because any deposit is associated to the jamming of the bottom opening. Thus, waiting until half of the basin is filled to clean the latter enable series of low-magnitude events to fill it. Coming more often permits the bottom opening to be cleaned, thus allowing subsequent low-magnitude event to pass through. Overall, the simulations are very consistent with the field observations that this debris basin is rapidly filled and cleaning operations have to be carried out often.

#### 4.2.2. Optimization of Maintenance Efficiency

The previous maintenance optimization takes into consideration only the cost of the maintenance strategy. However, decisions are not only made based on economic constraints but also on the efficiency of the maintenance strategy to increase the efficacy of the retention system in providing protection. In order to carry out such analysis, a comparison between the volumes released out of the retention dam depending on the adopted maintenance strategy should be performed. For this purpose, seven debris flow events of different input volumes corresponding to different return periods are extracted from the “Frequency - Magnitude” curve of fig. 8 and modeled separately using the physics-based model in order to obtain the output volume  $V_{out}$  of each. The input volumes  $V_{event}$  of the chosen events are 200, 11,000, 27,000, 35,000, 41,000, 46,000 and 49,000  $m^3$  corresponding to return periods of 1.1, 2, 5, 10, 20, 50 and 100 years, respectively. Each event is modeled in four different situations corresponding to four different initial stored volumes in the basin. These initial stored volumes  $V_{init}$  in each situation are assumed to be equal to the threshold volumes corresponding to the transition between the different defined states of the debris basin as follows:

*Situation 1:*  $V_{init} = 0 m^3$  (empty basin  $\rightarrow$  state 1)

*Situation 2:*  $V_{init} = 2,200 m^3$  (state 1  $\rightarrow$  state 2)

*Situation 3:*  $V_{init} = 10,000 m^3$  (state 2  $\rightarrow$  state 3)

*Situation 4:*  $V_{init} = 20,000 m^3$  (state 3  $\rightarrow$  state 4)

Furthermore, since the physics-based model involves a stochastic sub-model concerning the number of boulders jamming the openings of the dam (binomial law), 100 simulations were performed with each event and each initial filling to record an average value of the debris flow volume released downstream of the basin  $V_{out}$ .

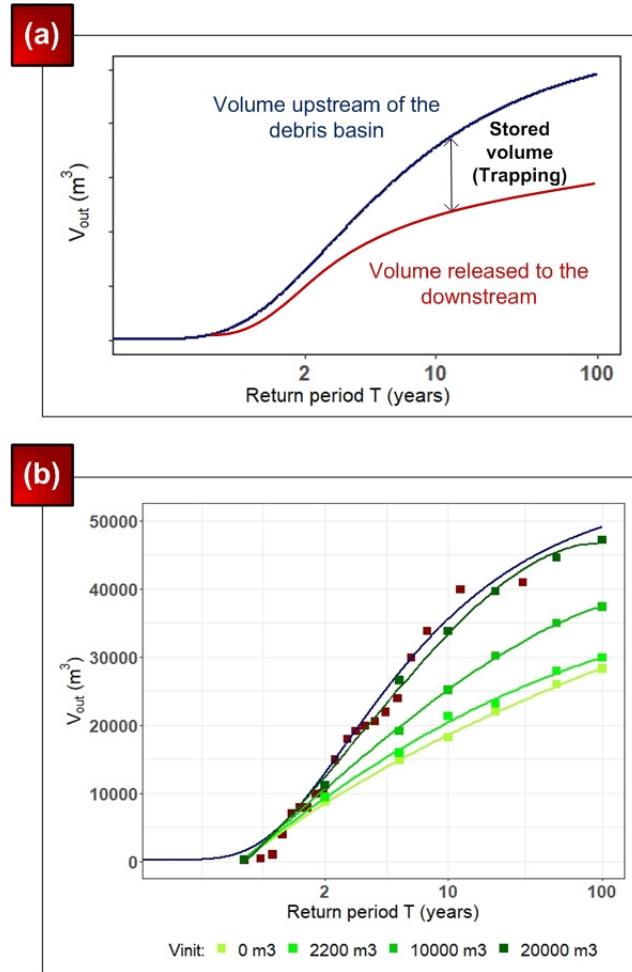


**Figure 15:** (a) Conceptual visualization of the protection efficacy across a wide range of events: Frequency - Magnitude of debris flow volumes supplied by the catchment (top line) and released downstream of the basin (bottom line). The difference between both line is a proxy of the protection efficacy for the associated return period; (b) Frequency - Magnitude curves presenting the output volumes of different debris flow events depending on the initial volume stored in the Claret's debris basin. The upper curve (in blue) is Claret's Frequency - Magnitude curve, which provides the volumes of debris flow events.

Fig. 15 represents the “Frequency - Magnitude” curve of the Claret torrent where the magnitudes in this case correspond to the output volumes  $V_{out}$ . The curve in blue is the one represented in fig. 8, which is fitted on the observed volumes (red squares). In the absence of the debris basin, it would correspond to the input volumes  $V_{event}$  that would be delivered to the downstream elements at risk. The four green curves in fig. 15 provide  $V_{out}$  for the considered debris flow events when considering the four situations of filling (initial volume stored in the basin  $V_{init}$ , the darker the green, the higher  $V_{init}$ ). In other words, in a given filling state, the debris basin on average transforms the process from the blue curve toward the associated green curve. It's important to highlight that the blue curve and the green curves have distinct starting points. The blue curve forms a continuous representation (GPD fitting) derived from historical databases, capturing the input volumes of debris flow events. In contrast, the green curves are constructed from seven discrete data points, each representing the output volume of a specific event generated by the developed model. These discrete points were then connected to create a smooth curve using a linear model implemented in R. From the obtained results, it is revealed that the higher  $V_{event}$  is, the higher  $V_{out}$  is (all curves are increasing to the right, i.e., toward higher return period). In addition, the higher  $V_{init}$  is, the higher  $V_{out}$  is (curves are sorted by green shading). Since  $V_{out}$  is the volume escaping the retention dam and transported to the downstream where vulnerable exposed issues are located, fig. 15 reveals the protection efficacy provided by Claret's retention system in different situations.

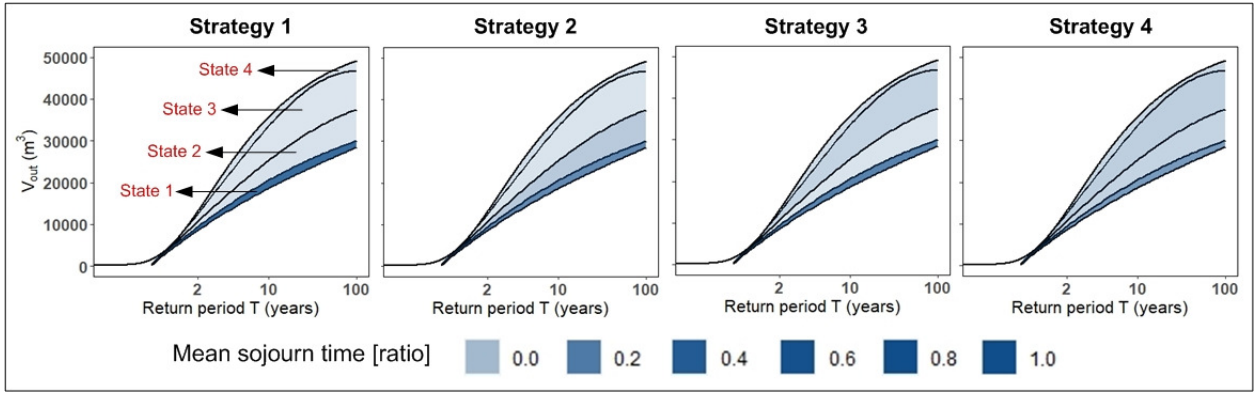


**Figure 16:** Maintenance efficiency revealed by the mean sojourn time (ratio) of the Claret's debris basin in each state based on the adopted strategy.

**Table 7**

Mean sojourn time (%) of the Claret's debris basin in each state depending on the adopted maintenance strategy.

Strategy	State 1 ( $\alpha * 100$ )	State 2 ( $\beta * 100$ )	State 3 ( $\gamma * 100$ )	State 4 ( $\theta * 100$ )
1	81	7	5	7
2	62	22	6	10
3	67	6	16	11
4	51	16	19	14

This representation of protection efficacy showing the frequency – magnitude curves upstream and downstream of the protection system was originally proposed by Hübl (2018). However, the latter did not consider the effect of maintenance strategies on increasing (or decreasing) the protection efficacy of the studied system. Fig. 15 provides transition curves that separate between the filling states of the debris basin. In order to analyze the efficiency of each maintenance strategy, the SPN model results concerning the mean sojourn time of the debris basin in each of the defined states under the adopted maintenance strategy should be considered, see table 5. They can be used to estimate the percentage of time spent by the basin in each filling state for each maintenance strategy, which corresponds at steady state to the probability (sojourn time in percentage) to have the corresponding initial filling level at the onset of an event. Since the efficacy of the basin is directly linked to its initial filling, it is thus possible to estimate the probability of being in a given level of efficacy over time. The sojourn time ratios  $\alpha$ ,  $\beta$ ,  $\gamma$  and  $\theta$ , representing the portion of time the system spends in specific states relative to the total simulation duration (50 years), are provided in Table 7. These ratios make it possible to characterize the efficacy of the system under the adopted maintenance strategy. Fig. 16 incorporates the curves obtained in fig. 15 and provides a graphical representation of the initial filling state probability (or sojourn times ratios) given in table 7. A color scale is used in order to differentiate between the times spent by the basin in each state, in which the darker the color is, the more probable the basin is in a given state. The lower domain of state 1 (almost empty basin) is darker for strategy 1, i.e., the basin is more often in this state than in the other strategies, while, at the other end of the spectrum, strategy 4 leads to a more frequently partially filled basin (darker intermediate states) and thus a more infrequently empty basin (clearer bottom domain). The efficacy of the four maintenance strategies can then be visually interpreted, through this potential transformation of an incoming event into a buffered outlet volume related to the more or less frequent initial state of filling when comes the event.

The protection efficacy of a debris retention system is mainly a matter of how much debris volume is released to the downstream  $V_{out}$ . This depends on the volume of the debris flow event  $V_{event}$  and on the initial state of filling of the basin  $V_{init}$  before the occurrence of the event. In order to reduce maintenance costs, the main challenge is to maximize  $V_{out}$  and to minimize the volume stored in the basin  $V_b$  while considering downstream protection needs. On the other hand, in order to increase the protection efficacy of the retention system, the challenge is to minimize  $V_{out}$  above the threshold

**Table 8**

Average total cost (k€) of each of the defined maintenance strategies for  $T_5 = 0.5$  years and  $T_5 = 2$  years. The given percentages correspond to the differences with the values provided when considering  $T_5 = 1$  year.

	Maintenance strategy			
	1	2	3	4
$T_5 = 1$	480	484	449	441
$T_5 = 0.5$	482 +0.3%	499 +3%	458 +2%	450 +2%
$T_5 = 2$	435 -9%	441 -9%	401 -11%	396 -10%

of dangerous events (below this threshold, no flooding occurs and debris flows should, if possible, be transferred to the downstream without interfering). The issue consists then in deciding whether it is acceptable to take risk and to keep the basin residing for more time at a lower level of efficacy (i.e., higher on the curves of fig. 15) or to pay more while guaranteeing a high level of protection efficacy. These two objectives are obviously in conflict, and the managers of the system have to find a trade-off between maintenance costs and protection efficacy. The information provided by the proposed model, as shown in Figs. 14 and 16, is relevant to identify a desired balance between maintenance costs and protection efficacy and can be leveraged to support the managers' maintenance decision-making. For example, when two strategies have similar costs (e.g., strategies 1 and 4) but they provide highly different levels of protection, managers can choose to invest the cost difference and select the one that provides a higher level of protection (strategy 1).

### 4.3. Sensitivity Analysis: Uncertainties Affecting Maintenance Decisions

Although the modeling and analysis of the Claret retention system are based on real data, the data used could still be imperfect, invaded by uncertainties or based on expert assessments. Therefore, it is worth exploring different situations under a given set of assumptions. In this section, a simple sensitivity analysis is performed considering different parameters that could affect maintenance decisions. The objective is not only to test the robustness of our analysis but also to improve decision-making in case something changes in the future (e.g., easier maintenance operations, more expensive operations). Three different parameters are chosen for this purpose: frequency of inspection, maintenance duration and maintenance costs.

#### 4.3.1. Inspection Frequency

In the previous modeling, it was assumed that inspection takes place once per year ( $T_5 = 1$  year). In other words, the state of the basin is considered only one time per year whatever the number of events that have already occurred within the year. Therefore, a decision concerning maintenance is only taken once per year. Simulations using the SPN model are carried out again considering two other inspection times ( $T_5 = 0.5$  years and  $T_5 = 2$  years). Results concerning the mean sojourn time of the basin in each state and the average number of maintenance operations performed over a period of 50 years are obtained. It is revealed that for  $T_5 = 0.5$  years, the times spent by the basin in the different states did not differ much than those corresponding to  $T_5 = 1$  year (< 14 % difference). Similarly for the number of maintenance operations carried out over a duration of 50 years (< 8 % difference). However, for  $T_5 = 2$  years, the percentage difference was higher for both the mean sojourn time (up to 70 %) and for the applied maintenance operations (up to 25 %). This can be justified by the fact that in the Claret, debris flows are triggered maximum once per year and more probably once every 2 years. Hence, inspecting every 0.5 years has quite the same efficiency as inspecting once per year. On the other hand, inspecting once every 2 years may not be as efficient as inspecting once per year since one triggered debris flow may be missed and thus the basin will spend more time in the same state or will evolve into a more deteriorated state without doing any preventive maintenance.

The total average costs of the defined maintenance strategies, for each inspection time, are provided in table 8. Note that the table involves also the percentage difference with the resulting values corresponding to the initial case where the inspection time is  $T_5 = 1$  year. Although results regarding the mean sojourn time and the average number of applied maintenance operations for  $T_5 = 1$  years show a slight difference with  $T_5 = 0.5$  years and a considerable difference with  $T_5 = 2$  years, the total costs of the maintenance strategies have not shown a big difference (up to

3 % for  $T_5 = 0.5$  years and up to 10 % for  $T_5 = 2$  years). Nonetheless, for all the considered times of inspection, maintenance strategy 4 remains the most cost-effective regardless that the costs of all strategies show a very slight difference.

#### 4.3.2. Maintenance Duration

As mentioned in section 3.2.3, the scheduling duration of maintenance is assumed to be 2.5 months for all the considered operations and the time to clean the basin depends on the debris volume to be cleaned: 1 month for minor operations, 2 months for major operations and 3 months for corrective operations. The chosen duration may vary depending on different situations. For example, in the case where enough funds are available, maintenance contracts can be made with companies in concern with these systems. In such a case, the scheduling time of maintenance will be much less than the one considered since there is no need to search, ask and wait for funding to apply the maintenance operation. Instead, maintenance is applied as soon as it is requested. In addition, in the case where large boulders are deposited in the basin, the time to carry out maintenance may vary depending on the capacity of the engines and on the distance traveled to reach the location where the deposits are evacuated. Therefore, the duration needed to perform the maintenance operation is not only dependent on the volume to be cleaned.

In the case of having a maintenance contract (case 1), the duration of maintenance is assumed to be faster by about two and a half months as follows:

- Minor operations: 1 week + 1 month
- Major operations: 1 week + 2 months
- Corrective operations: 1 week + 3 months

On the other hand, in the case when large boulders are present and the distance to evacuation is quite long (case 2), the duration of maintenance is assumed to increase by one month as follows:

- Minor operations: 2.5 months + 2 months
- Major operations: 2.5 months + 3 months
- Corrective operations: 2.5 months + 4 months

In both cases, the first duration corresponds to the scheduling time of the operation and the other corresponds to the time needed to carry out the maintenance (cleaning) operation. Note that these constant delay times are assigned to the deterministic transitions involved in the maintenance process of the SPN model ( $T_9$ ,  $T_{10}$  and  $T_{11}$ ). The 200 simulations of the SPN model provide results concerning the mean sojourn time of the basin in each state and the average number of maintenance operations performed over a period of 50 years. For each case, the obtained results are compared with those corresponding to the initial analyzed case (noted "case 0"). In case 1, the time spent by the basin in each state shows a significant difference (up to 30 % difference) when compared to those corresponding to the initial case. Concerning the number of maintenance operations, the difference between the results is low (< 8 % difference). In case 2, the percentage difference was also high for the mean sojourn time (up to 20 %) but less than those attained in case 1. This can be justified by the fact that, in the initial case, maintenance operations need about 1.5 months more time than in case 1 to be carried out but only 1 month less time than in case 2. Consequently, results corresponding to case 2 will be closer to those of the initial case than those of case 1. Moreover, it is also noticed that in case 1, the time spent by the basin in state 1 is higher than that when applying case 2 or the initial case in all strategies. This is due to the fast-performed maintenance operations that return the basin back to its initial good state. For the number of applied maintenance operations, case 2 did not result in a big difference when compared to the initial case (up to 8 %).

The total costs of the different maintenance strategies, given in table 9, did not differ much in both cases as they are proportional to the number of performed operations. Still, maintenance strategy 4 remains the most cost-effective.

#### 4.3.3. Maintenance Costs

The costs of maintenance operations previously used in the model are estimated depending on the debris volume to be cleaned ( $2.83 \text{ €/m}^3$ ). The debris volume corresponding to each state of the basin is assumed to be equal to the average of the two threshold volumes defining the state. As given in table 4, the average costs of minor, major and corrective operations are, respectively, 17 k€, 42 k€ and 59 k€. In order to check the influence of varying the costs of maintenance operations on the total cost of the defined maintenance strategies, a simple example that accounts for this variation is considered in this study. Instead of considering only the average volumes of the intervals defining the

**Table 9**

Average total cost (k€) of each of the defined maintenance strategies for case 1 and case 2 maintenance duration. The given percentages correspond to the differences with the values provided when considering the initial maintenance duration.

	Maintenance strategy			
	1	2	3	4
Case 0	480	484	449	441
Case 1	498 +4%	505 +4%	463 +3%	456 +3%
Case 2	462 -4%	470 -3%	430 -4%	427 -3%

states, three different volumes (minimum, average and maximum values) are considered. Below are the equations used to estimate the costs of the minor, major and corrective operations depending on the volume to be cleaned.

*Minor operation:*  $V_b \in [2200, 10000[$

$$- V_{2200}: C_{2200} = 2200 \text{ m}^3 * 2.83 \text{ €/m}^3 \approx 6 \text{ k€}$$

$$- V_{6100}: C_{6100} = 6100 \text{ m}^3 * 2.83 \text{ €/m}^3 \approx 17 \text{ k€}$$

*Major operations:*  $V_b \in [10000, 20000[$

$$V_{10000}: C_{10000} = 10000 \text{ m}^3 * 2.83 \text{ €/m}^3 \approx 28 \text{ k€}$$

$$V_{15000}: C_{15000} = 15000 \text{ m}^3 * 2.83 \text{ €/m}^3 \approx 42 \text{ k€}$$

*Corrective operations:*  $V_b \in [20000, 22000]$

$$V_{20000}: C_{20000} = 20000 \text{ m}^3 * 2.83 \text{ €/m}^3 \approx 57 \text{ k€}$$

$$V_{21000}: C_{21000} = 21000 \text{ m}^3 * 2.83 \text{ €/m}^3 \approx 59 \text{ k€}$$

$$V_{22000}: C_{22000} = 220000 \text{ m}^3 * 2.83 \text{ €/m}^3 \approx 62 \text{ k€}$$

The main objective is to create several configurations and to check the total costs of the defined maintenance strategies based on the number of applied maintenance operations carried out over a period of 50 years. The results of the SPN model presented in table 6 are used for this purpose. For simplicity, only four different configurations are chosen:

*Configuration 1:* minor, major and corrective operations are applied, respectively, for  $V_b = V_{2200}$ ,  $V_b = V_{10000}$  and  $V_b = V_{20000}$ .

*Configuration 2:* minor, major and corrective operations are applied, respectively, for  $V_b = V_{2200}$ ,  $V_b = V_{10000}$  and  $V_b = V_{22000}$ .

*Configuration 3:* minor, major and corrective operations are applied, respectively, for  $V_b = V_{6100}$ ,  $V_b = V_{10000}$  and  $V_b = V_{21000}$ .

*Configuration 4:* minor, major and corrective operations are applied, respectively, for  $V_b = V_{2200}$ ,  $V_b = V_{15000}$  and  $V_b = V_{22000}$ .

For each configuration, multiplying the cost of each operation with the number of performed operations (table 6), provides the total cost of each maintenance strategy. Results are provided in table 10.

From the obtained results, it can be realized that the total costs of maintenance strategies significantly differ depending on the adopted configuration. This variation arises because, in each configuration, the volume to be cleaned in each state varies, subsequently influencing the cost associated with each maintenance operation performed. Indeed, the resulting difference affects the sorting of the maintenance strategies and thus the maintenance decision. For configurations 1 and 2, strategy 1 is the most cost-effective and strategy 4 is the most expensive. In the contrary, for configuration 3, strategy 2 is the most cost-effective and strategy 3 is the most expensive. With regards to configuration

**Table 10**

Average total cost (k€) of each of the defined maintenance strategies for the four proposed configurations. The given percentages correspond to the differences with the values provided when considering the reference configuration considered in section 3.2.3 (noted "0").

	Maintenance strategy			
	1	2	3	4
Configuration 0	480	484	449	441
Configuration 1	367 -23%	416 -14%	391 -13%	426 -3%
Configuration 2	388 -19%	443 -9%	423 -6%	463 +5%
Configuration 3	429 -11%	427 -12%	449 -	441 -
Configuration 4	439 -8%	450 -3%	424 -2%	463 +5%

4, strategy 3 is the most cost-effective and strategy 2 is the most expensive. However, for the initial considered configuration, strategy 4 is the most cost-effective and strategy 2 is the most expensive. The variability in the results highlights the importance of considering the costs of cleaning operations depending on the actual volume stored in the basin instead of considering an average volume. Indeed, the overall decision-making model seems to be very sensitive to the costs of maintenance operations relative to the volume stored in the basin. Consequently, deep attention should be given when collecting information about the debris volume stored in the basin. This will apparently better support decision-makers to undertake optimal maintenance decisions.

## 5. Concluding remarks

In this study, a scenario-driven physics-based model is developed to model the evolution of the debris volume stored in a basin over time. The end purpose of this model is to provide deterioration trajectories that make it possible to learn probability laws corresponding to the transition times between the defined states of the basin. A surrogate capacity deterioration model that uses the information provided by the physics-based model is then developed using SPNs. The model facilitates implementing a CBM policy concerning cleaning operations of the basin and assessing its performance. The outputs of the SPN model support the managers of retention systems to optimize different maintenance strategies in terms of cost and efficiency. The overall developed modeling approach is used to analyze the performance of the retention system located in the Claret torrent in France. The complete framework is particularly interesting because it enables fast explorations of the various maintenance policies and facilitates performing sensitivity analyses without requiring to run many times a sophisticated physics-based model: computations on the physics-based model are done considering no maintenance, and a surrogate model is then learned and complemented by integrating maintenance operations making it possible to explore the effect of maintenance. Optimizing maintenance while ensuring satisfying protection efficacy is the dual objective of the managers of these structures. In this paper, we suggest in fig. 16 a new way to visualize the effect of a maintenance strategy on the protection efficacy of debris basins.

### 5.1. Main Findings

The achieved results make it possible to analyze the contributions behind this work according to different points of view. From a thematic point of view related to debris retention systems, the developed approach provides a new dynamic vision of their management over time. It models the discharge buffering and debris trapping effects of the system over time, the probability that the dam will trap boulders and how much it will cost to perform cleaning operations depending on the debris volume stored in the basin. From a research point of view, the developed approach reflects the real behavior of a deteriorating retention system by coupling physics-based modeling of the deterioration process and reliability-based modeling for maintenance assessment based on a SPN model integrating CBM operations. It proposes a global methodology for implementing SPNs with an original contribution that aims at determining and

justifying the probability laws corresponding to the transition times between different states of the debris basin. From an operational/technical point of view, the developed approach contributes to a better and more resilient management: knowing what can happen and being somehow better prepared to unavoidable evolution of the retention system, risk managers can better anticipate and take optimal decisions.

Note that the developed approach can end up by making different maintenance decisions depending on the configuration of the site under study.

## 5.2. Perspectives and Future Work

Regardless of the originality and the contributions of the present work, more research is required in order to cover some limitations. For example, the thresholds corresponding to the defined deterioration states are crucial elements and should be carefully selected. In this study, these thresholds are chosen based on expert assessment but still require verification. Moreover, the consequences identified after a debris flow do not take into account the risk imposed on the downstream exposed issues (elements at risk). Besides, the inflation rate of prices is not accounted for in this study, in which maintenance costs are assumed to be constant over time ( $2.83 \text{ €}/\text{m}^3$ ). To sum up, the cost model adopted in this research work is not sophisticated enough. Accordingly, future work can involve:

- Carrying out more research and technical analysis in order to better choose the deterioration states' thresholds.
- Estimating the risk imposed on downstream elements by collecting data concerning the type of exposed elements and assessing their vulnerability.
- Taking into account the monetary evolution over time instead of constant maintenance costs. This can be done by incorporating in the cost model either an inflation rate or a discount rate.

## Acknowledgments

This work has been partially supported by MIAI@Grenoble Alpes, (ANR-19-P3IA-0003). We also thank our colleagues from ONF/RTM in Savoy department and natural risk directorate for data provision and fruitful discussions and collaboration.

## References

- Alaswad, S., Xiang, Y., 2017. A review on condition-based maintenance optimization models for stochastically deteriorating system. *Reliability Engineering & System Safety* 157, 54–63. URL: <http://www.sciencedirect.com/science/article/pii/S0951832016303714>.
- Armanini, A., Dellagiacomma, F., Ferrari, L., 1991. From the check dam to the development of functional check dams., in: Armanini, A., Di Silvio, G. (Eds.), *Fluvial Hydraulics of Mountain Regions.*, Springer Berlin Heidelberg, Berlin, Heidelberg. pp. 331–344.
- Asghari, V., Hsu, S.C., 2021. An open-source and extensible platform for general infrastructure asset management system. *Automation in Construction* 127, 103692. doi:<https://doi.org/10.1016/j.autcon.2021.103692>.
- Aubry, J.F., Brinzei, N., Mazouni, M.H., 2016. Systems Dependability Assessment: Benefits of Petri Net Models. volume 1 of *Systems and Industrial Engineering Series. Systems Dependability Assessment Set*. ISTE Ltd and John Wiley & Sons Inc. URL: <https://hal.archives-ouvertes.fr/hal-01320631>.
- Badoux, A., Andres, N., Turowski, J., 2014. Damage costs due to bedload transport processes in Switzerland. *Natural Hazards and Earth System Sciences* 14, 279–294. doi:10.5194/nhess-14-279-2014.
- Biondini, F., Frangopol, D.M., 2016. Life-cycle performance of deteriorating structural systems under uncertainty: Review. *Journal of Structural Engineering* 142, F4016001. doi:10.1061/(ASCE)ST.1943-541X.0001544.
- Bonczek, R.H., Holsapple, C.W., Whinston, A.B., 1981. *Foundations of Decision Support Systems*. Number 9780121130503 in Elsevier Monographs, Elsevier.
- Callow, D., Lee, J., Blumenstein, M., Loo, Y.C., 2012. Development of hybrid optimisation method for artificial intelligence based bridge deterioration model — feasibility study. *Automation in Construction* 31, 83–91. doi:10.1016/j.autcon.2012.11.016.
- Carladous, S., Piton, G., Kuss, D., Charvet, G., Paulhe, R., Morel, M., Queffélec, Y., 2022. Check Dam Construction for Sustainable Watershed Management and Planning. Wiley Online Library. chapter 13: French Experience with Open Check Dams: Inventory and Lessons Learnt Through Adaptive Management. pp. 247–266.
- Chahrour, N., Nasr, M., Tacnet, J.M., Bérenguer, C., 2021. Deterioration modeling and maintenance assessment using physics-informed stochastic petri nets: Application to torrent protection structures. *Reliability Engineering & System Safety* 210, 107524. doi:<https://doi.org/10.1016/j.res.2021.107524>.
- Coussot, P., Meunier, M., 1996. Recognition, classification and mechanical description of debris flows. *Earth-Science Reviews* 40, 209–227. doi:10.1016/0012-8252(95)00065-8.
- Deymier, C., Tacnet, J.M., Mathys, N., 1995. *Conception et calcul de barrages de correction torrentielle*. Grenoble, France: Cemagref Editions, 287p. [In French].

- Ferreira, C., Canhoto Neves, L., Silva, A., de Brito, J., 2018. Stochastic petri net-based modelling of the durability of renderings. *Automation in Construction* 87, 96–105. doi:<https://doi.org/10.1016/j.autcon.2017.12.007>.
- Guler, H., 2013. Decision support system for railway track maintenance and renewal management. *Journal of Computing in Civil Engineering* 27, 292–306. doi:10.1061/(ASCE)CP.1943-5487.0000221.
- Hilker, N., Badoux, A., Hegg, C., 2009. The Swiss flood and landslide damage database 1972–2007. *Natural Hazards and Earth System Sciences* 9, 913–925. doi:10.5194/nhess-9-913-2009.
- Hübl, J., Strauss, A., Holub, M., Suda, J., 2005. Structural Mitigation Measures., in: *Proceedings zum 3rd Probabilistic Workshop: Technical Systems + Natural Hazards*, 24–25 November, Wien.
- Hugerot, T., 2015. Etude des trajectoires paysagères et des dynamiques anthropoclimatiques des cônes de déjection torrentiels dans les alpes du nord: l'exemple du cône de déjection du claret en maurienne. *Univ. Savoie Mont Blanc*.
- Hübl, J., 2018. Conceptual framework for sediment management in torrents. *Water* 10. doi:10.3390/w10121718.
- Hübl, J., Suda, J., 2008. Debris flow mitigation measures in Austria., in: *Debris Flows: Disaster, Risk, Forecast, Protection*. Pyatigorsk, Russia.
- Ikeya, H., 1989. Debris flow and its countermeasures in japan. *Bulletin - International Association of Engineering Geology* 40(1): 15–33. .
- Kaplan, E.L., Meier, P., 1958. Nonparametric estimation from incomplete observations. *Journal of the American Statistical Association* 53, 457–481. URL: <http://www.jstor.org/stable/2281868>.
- Le, B., Andrews, J., Fecarotti, C., 2017. A petri net model for railway bridge maintenance. *Proceedings of the Institution of Mechanical Engineers, Part O: Journal of Risk and Reliability* 231, 306–323. doi:10.1177/1748006X17701667.
- Mizuyama, T., Kobashi, S., Ou, G., 1992. Prediction of debris flow peak discharge, in: *INTERPRAEVENT*, Vol. 4, International Research Society INTERPRAEVENT, Bern, Switzerland. p. 99–108.
- Morel, M., Piton, G., Evin, G., Le Bouteiller, C., 2022. *Projet HYDRODEMO : Évaluation de l'aléa torrentiel dans les petits bassins versants des Alpes du Nord*. Research Report. INRAE. URL: <https://hal.archives-ouvertes.fr/hal-03549827>.
- ONF-RTM, 2013. *Études de bassin versant: Torrent du Claret*. Research report. Office National des Forêts, Service de Restauration des Terrains en Montagne du Département de l'Isère, Grenoble. [In French].
- Pan, Y., Zhang, L., 2021. Roles of artificial intelligence in construction engineering and management: A critical review and future trends. *Automation in Construction* 122, 103517. doi:<https://doi.org/10.1016/j.autcon.2020.103517>.
- Paulhe, R., Kuss, D., Lamy, O., Etcheverry, D., Carladous, S., Martin, R., 2018. Retour d'expérience sur les travaux de modification de la plage de dépôt du Claret (73). Research report. Office National des Forêts, Service de Restauration des Terrains en Montagne du Département de l'Isère, Grenoble, ONF-RTM Agence Rhône Alpes. [In French].
- Petri, C.A., 1962. *Kommunikation mit Automaten*. Bonn: Mathematisches Institut der Universität Bonn. [In German].
- Piton, G., Carladous, S., Recking, A., Liebault, F., Tacnet, J., Kuss, D., Quefféléan, Y., Marco, O., 2017. Why do we build check dams in Alpine streams? An historical perspective from the French experience. *Earth Surface Processes and Landforms* 42, 91–108. doi:10.1002/esp.3967.
- Piton, G., Fontaine, F., Bellot, H., Liébault, F., Bel, C., Recking, A., Hugerot, T., 2018. Direct field observations of massive bedload and debris-flow depositions in open check dams. *E3S Web of Conferences* 40, 8 p. doi:10.1051/e3sconf/20184003003.
- Piton, G., Goodwin, S.R., Mark, E., Strouth, A., 2022. Debris flows, boulders and constrictions: a simple framework for modeling jamming, and its consequences on outflow. *Journal of Geophysical Research: Earth Surface* doi:<https://doi.org/10.1029/2021JF006447>.
- Piton, G., Recking, A., 2015. Design of Sediment Traps with Open Check Dams. I: Hydraulic and Deposition Processes. *Journal of Hydraulic Engineering* 142, 1–16. doi:10.1061/(ASCE)HY.1943-7900.0001048.
- Russell, S., Norvig, P., 2020. *Artificial Intelligence: A Modern Approach*. 4th Edition, Boston : Pearson.
- Sanders, W.H., Meyer, J.F., 2001. Stochastic activity networks: Formal definitions and concepts, in: Brinksma, E., Hermanns, H., Katoen, J.P. (Eds.), *Lectures on Formal Methods and Performance Analysis: First EEF/Euro Summer School on Trends in Computer Science*, Bergen Dal, The Netherlands, July 3–7, 2000 - Revised Lectures. Springer, Berlin, Heidelberg, pp. 315–343. doi:10.1007/3-540-44667-2\_9.
- Signoret, J.P., 2009. Dependability & safety modeling and calculation: Petri nets. *IFAC Proceedings Volumes* 42, 203 – 208. doi:<https://doi.org/10.3182/20090610-3-IT-4004.00040>. 2nd IFAC Workshop on Dependable Control of Discrete Systems.
- Tao, W., Lin, P., Wang, N., 2021. Optimum life-cycle maintenance strategies of deteriorating highway bridges subject to seismic hazard by a hybrid markov decision process model. *Structural Safety* 89, 102042. doi:<https://doi.org/10.1016/j.strusafe.2020.102042>.
- Wang, C., Yu, Q., Law, K.H., McKenna, F., Yu, S.X., Taciroglu, E., Zsarnóczy, A., Elhaddad, W., Cetiner, B., 2021. Machine learning-based regional scale intelligent modeling of building information for natural hazard risk management. *Automation in Construction* 122, 103474. doi:<https://doi.org/10.1016/j.autcon.2020.103474>.
- Yang, D.Y., Frangopol, D.M., 2019. Life-cycle management of deteriorating civil infrastructure considering resilience to lifetime hazards: A general approach based on renewal-reward processes. *Reliability Engineering & System Safety* 183, 197–212. doi:10.1016/j.res.2018.11.016.
- Yang, J., Xiang, F., Li, R., Zhang, L., Yang, X., Jiang, S., Zhang, H., Wang, D., Liu, X., 2022. Intelligent bridge management via big data knowledge engineering. *Automation in Construction* 135, 104118. doi:<https://doi.org/10.1016/j.autcon.2021.104118>.
- Yianni, P.C., Rama, D., Neves, L.C., Andrews, J.D., Castlo, D., 2017. A Petri-Net-based modelling approach to railway bridge asset management. *Structure and Infrastructure Engineering* 13, 287–297. doi:10.1080/15732479.2016.1157826, arXiv:<https://doi.org/10.1080/15732479.2016.1157826>.
- Zimmermann, A., 2008. *Stochastic Discrete Event Systems: Modeling, Evaluation, Applications*. Springer, Berlin, Heidelberg. chapter Colored Petri Nets. pp. 99–124. doi:10.1007/978-3-540-74173-2\_6.
- Zollinger, F., 1983. *Die Vorgänge in einem Geschiebeablagungsplatz (ihre Morphologie und die Möglichkeiten einer Steuerung)*. Phd. theses. ETH Zürich. doi:<https://doi.org/10.3929/ethz-a-000318964>. [In German].
- Zollinger, F., 1985. Debris detention basins in the European Alps., in: *International symposium on Erosion, Debris Flow and Disaster Prevention*. Tsukuba, Japan: Japan Erosion Control Engineering Society., pp. 433–438.
- Šelih, J., Kne, A., Srđić, A., Žura, M., 2008. Multiple-criteria decision support system in highway infrastructure management. *Transport* 23, 299–305. doi:10.3846/1648-4142.2008.23.299-305.